State of California
California Natural Resources Agency
DEPARTMENT OF WATER RESOURCES

Travel Time and Longitudinal Dispersion Rates in the California State Water Project

December 2012

Edmund G. Brown Jr.
Governor
State of California

John Laird
Secretary
Natural Resources Agency

Mark W. Cowin
Director
Department of Water Resources

Foreword

The California Aqueduct supplies drinking water to millions of Californians. The aqueduct also provides water for the agricultural effort in California's Central Valley which in turn supplies food for the entire nation. We know a great deal about how much water the aqueduct is capable of transporting; however, we know little about the hydrologic conditions within the aqueduct. Knowledge of these hydrologic conditions within the aqueduct is required to address water quality concerns that arise and is critical during emergency and hazardous spill response. This study was designed to answer questions related to travel time and longitudinal dispersion within the California Aqueduct.

This study was initiated to determine if the models being developed by the Department of Water Resources accurately predicted travel times and rates of dispersion within the California Aqueduct. The Department's Municipal Water Quality Investigations Section (MWQI) Special Studies Work Group requested this investigation be added to the MWQI workplan in 2006. This report is the second of two phases. Phase 1 data collection took place in the summer of 2008 and a report was completed the following year.

Table of Contents

Tables

Figures

Photo Credits

Photos taken by Jason Moore

State of California
Edmund G. Brown Jr., Governor

California Natural Resources Agency
John Laird, Secretary for Natural Resources

Department of Water Resources
Mark W. Cowin, Director

Susan Sims, Chief Deputy Director

Office of the Chief Counsel Cathy Crothers	Public Affairs Office Nancy Vogel, Communications Dir.	Security Operations Sonny Fong
Government & Community Liaison Kimberly Johnston-Dodds	Policy Advisor Waiman Yip	Legislative Affairs Office Kasey Schimke, Assistant Dir.

Deputy Directors

Dale Hoffman-Floerke — **Delta and Statewide Water Management**
Assistant to Deputy Director: B Harrell and B Heiland

Gary Bardini — **Integrated Water Management**
Assistant to Deputy Director J Marr; Assistant Deputy Director J Andrew, Climate Change

Carl Torgersen, acting — **State Water Project**
Assistant to Deputy Director: P Lecocq and G Scholl; Assistant Deputy Director M Anderson

John Pacheco, acting — **California Energy Resources Scheduling**
Assistant to Deputy Director R. Grix

Kathie Kishaba — **Business Operations**
Assistant to Deputy Director S. Varrelman

Division of Environmental Services
Dean F. Messer, Chief

Office of Water Quality
Stephani A. Spaar, Chief

Prepared under the supervision of

Municipal Water Quality Program Branch
Cindy Garcia, Chief

Prepared by

Jason Moore ..... Environmental Scientist

Ted Swift ..... Staff Environmental Scientist

Editorial review, graphics, and report production

Under direction of Supervisor of Technical Publications Patricia Cornelius, research writers:

Mike Durant	Frank Keeley	Charlie Olivares	Carole Rains
Sarah Sol	Jeff Woled		Marilee Talley

Metric Conversions Table

Quantity	To convert from metric unit	To customary unit	Multiply metric unit ny	To convert to metric unit multiply customary unit by
Length	millimeters (mm)	inches (in)	0.03937	25.4
	centimeters (cm) for snow depth	inches (in)	0.3937	2.54
	meters (m)	feet (ft)	3.2808	0.3048
	kilometers (km)	miles (mi)	0.62139	1.6093
Area	square millimeters (mm^2)	square inches (in^2)	0.00155	645.16
	square meters (m^2)	square feet (ft^2)	10.764	0.092903
	hectares (ha)	acres (ac)	2.4710	0.40469
	square kilometers (km^2)	square miles (mi^2)	0.3861	2.590
Volume	liters (L)	gallons (gal)	0.26417	3.7854
	megaliters (ML)	million gallons (10*)	0.26417	3.7854
	cubic meters (m^3)	cubic feet (ft^3)	35.315	0.028317
	cubic meters (m^3)	cubic yards (yd^3)	1.308	0.76455
	cubic dekameters (dam^3)	acre-feet (ac-ft)	0.8107	1.2335
Flow	cubic meters per second (m^3/s)	cubic feet per second (ft^3/s)	35.315	0.028317
	liters per minute (L/mn)	gallons per minute (gal/mn)	0.26417	3.7854
	liters per day (L/day)	gallons per day (gal/day)	0.26417	3.7854
	megaliters per day (ML/day)	million gallons per day (mgd)	0.26417	3.7854
	cubic dekameters per day (dam^3/day)	acre-feet per day (ac-ft/day)	0.8107	1.2335
Mass	kilograms (kg)	pounds (lbs)	2.2046	0.45359
	megagrams (Mg)	tons (short, 2,000 lb.)	1.1023	0.90718
Velocity	meters per second (m/s)	feet per second (ft/s)	3.2808	0.3048
Power	kilowatts (kW)	horsepower (hp)	1.3405	0.746
Pressure	kilopascals (kPa)	pounds per square inch (psi)	0.14505	6.8948
	kilopascals (kPa)	feet head of water	0.32456	2.989
Specific capacity	liters per minute per meter drawdown	gallons per minute per foot drawdown	0.08052	12.419
Concentration	milligrams per liter (mg/L)	parts per million (ppm)	1.0	1.0
Electrical conductivity	microsiemens per centimeter (µS/cm)	micromhos per centimeter (µmhos/cm)	1.0	1.0
Temperature	degrees Celsius (°C)	degrees Fahrenheit (°F)	(1.8X°C)+32	0.56(°F-32)

Executive Summary

The California Aqueduct supplies drinking water to millions of Californians. The aqueduct also provides water for the agricultural effort in California's Central Valley which in turn supplies food for the entire nation. We know a great deal about how much water the aqueduct is capable of transporting; however, we know little about the hydrologic conditions within the aqueduct. Knowledge of these hydrologic conditions within the aqueduct is required to address water quality concerns that arise and is critical during emergency and hazardous spill response. This study was designed to answer questions related to travel time and longitudinal dispersion within the California Aqueduct.

The first question answered by this study is, "How long does it take water to travel from one point in the aqueduct to another point?" or more specifically, "What is the velocity of water in the aqueduct?" The second question answered by this study is, "What is the rate of dispersion of water in the aqueduct?" According to Allaby and Allaby's 1999 *A Dictionary of Earth Sciences*, "longitudinal dispersion is the spreading out of a body of water along its own flow path, due to the differences in water velocities." Having an answer to these questions is useful for operators of the aqueduct when situations arise such as hazardous spills and algal blooms. Modelers also can use this data to fine tune models of the aqueduct water quality and operations.

These two questions were answered using a novel technique where an U.S. Environmental Protection Agency-approved fluorescent dye was released into the aqueduct. The invisible dye was detected using fluorometers placed at various locations along the aqueduct. The concentration of dye was recorded as the dye travelled with the water down the aqueduct. The signals produced by the dye gave precise information as to the arrival times and concentrations of the dye at each location.

With this dye travel data, accurate models were made that reflected the conditions seen in the aqueduct during our study period. These models were then used to determine that during this study average water velocity is 1.50 feet per second and the longitudinal dispersion rate is approximately 0.32 ft/s. In addition, an example of how to use this data is given at the end of the study report. Another interesting finding of this study was that at times water in the aqueduct reverses flow when upstream withdrawals are greater than the normal flow.

Introduction

A Municipal Water Quality Investigations (MWQI) study to quantify the travel time and longitudinal dispersion rate of water in the State Water Project's California Aqueduct (the aqueduct) was conducted in two phases. Phase 1 was completed in 2008 and a report on the findings was produced in June 2009. This report outlines phase 2—simultaneous release of dye and drifters—the motivation behind this element of the study and methods used and modifications made to the original study design.

Phase 1 consisted of a field study using inert, individually identifiable, neutrally buoyant drifters. It was thought that inert drifters would avoid questions and permitting required using a dissolved tracer, such as fluorescent dye. The study was performed on a 100-mile long section of the East Branch of the California Aqueduct in August 2008. Each drifter contained an acoustic transmitter (Vemco, Inc.) whose passage was recorded by acoustic receivers mounted in the aqueduct at intervals. Ten Vemco VR2R acoustic receiver/loggers were installed at known points along the study reach to record the time of passage of each of the drifters. While this study demonstrated that longitudinal dispersion was nonzero, there was also evidence of drifters being delayed or snagged. This raised questions about the ability of drifters to accurately represent dispersion rate and travel time of a dissolved substance in the aqueduct.

Phase 2 involved the simultaneous release of drifters and Rhodamine WT (RWT, Kingscote Chemicals) fluorescent dye into a section of the aqueduct downstream from the Check 14 flow control gates in July and August 2009. The dye and drifters were tracked for approximately 75 miles to just above Check 21. Methods for determining dispersion rates and travel times using dyes are well documented and commonly used (e.g., Fischer et al., 1979). The dye release was also used to prove or disprove the assumption that a set of neutrally buoyant drifters behaves essentially the same as a dissolved tracer.

The aqueduct's dispersion rate and travel times can be used by scientists, modelers, and engineers to predict concentration and arrival time of a constituent; for example, if a large amount of pesticide were spilled into the aqueduct at a point. With travel time and dispersion rate knowledge, it is possible to predict the following:

- whether the concentration of pesticide would dilute to safe levels at a downstream site,
- how long it would take the pesticide to travel to a downstream site,
- what quantity of water would be contaminated by the pesticide, and
- the concentration of the pesticide as it disperses.

In principle, a source location upstream can also be approximately located using detailed concentration information downstream. The same principles apply to other constituents in the water.

Phase 2 Study Motivation and Problem Definition

Phase 1 of the study used neutrally buoyant drifters and proved that the concept of tracking drifters through the use of acoustic tags is possible. However, analysis of phase 1 data suggested that the drifters could become impeded or captured by debris in the canal. The most striking example occurred with depth-sensing tag number 120. This tag traveled to within acoustic detection range of the first receiver shortly after the tag was launched. The tag apparently remained within detectable range of that receiver for more than two weeks while the other tags continued to travel downstream. This, along with depth data from one of the tags that contained a depth transponder, suggested that some of the dispersion seen among

the tags could be due to entanglement or other friction with the aqueduct perimeter, such as bouncing or "saltation," rather than the drifters following waterflow.

To address the ambiguous results produced by the drifter approach, MWQI staff added another element to the study, a fluorescent tracer dye and *in-situ* fluorometric devices that detect the concentration of the dye as it travels down the aqueduct. Techniques for determining dispersion rates in fluvial aquatic systems using tracer dyes are well established and have been widely accepted for many years (Kilpatrick, 1970, Fischer *et al.*, 1979).

As described in the first phase of this study from June 2009, at any given point of time after the release of dye and drifters into the aqueduct, dispersion theory suggests the particles should be distributed in roughly a Gaussian (bell-shaped) curve. The longitudinal dispersion coefficient is derived from the rate of change of the Gaussian's width with respect to time. The travel time can be measured as the time required for the leading edge, peak, etc. to travel a known distance. Actual studies performed by the U.S. Geological Survey (USGS) and others have shown that this curve has a shorter tail on the leading edge of the particle cloud and a longer tail on the trailing edge of the particle cloud (Hubbard *et al.*, 1982). This suggests that some of the tracer is delayed or "stored" in the channel roughness, especially important in natural streams. Kilpatrick and Wilson, in their 1989 revision paper, determined that, in order to get adequate data resolution, recording the concentrations of a trailing edge of a fluorescent dye cloud is only necessary until the concentration of the trailing edge is below 10% of the peak concentration.

Timeline of the Study

Preparations for the second phase of this study began in early January 2009 when concerns arose over whether a study involving only drifters could adequately answer the questions that the study was intended to resolve. Fluorescent tracer dye studies are the standard method for determining time of travel and dispersion rates in fluvial settings. After researching the health and safety aspects of RWT, it was determined that this approach was safe and feasible. Department of Water Resources (DWR) water quality specialists in the Division of Operations and Maintenance (O&M) were consulted by MWQI staff and agreed that the knowledge to be gathered from this study would be beneficial to many parties within DWR and to outside agencies. DWR branches worked together to coordinate with potential water users along the study section to ensure that all questions and concerns were addressed prior to the study.

The original deployment for this study was set for May of 2009; however, due to Delta pumping restrictions, flows in the aqueduct would be atypical during this period. Therefore, study dates were changed to the summer when flows were likely to be less restricted. The bulk of the data gathering portion of this study took place from July 27, 2009, until August 3, 2009. A single acoustic receiver was left at the study area downstream terminus for an additional 2 weeks to detect any straggling drifters.

Methods

The aqueduct travel time and longitudinal dispersion study executed the week of July 27, 2009, consisted of two simultaneous studies. Like the phase I study, the first element involved the placement of acoustic receivers along the aqueduct, followed by deployment of neutrally buoyant drifters (see “Drifter Study” in this report). The second element involved the insertion of a fluorescent tracer dye commercially known as Rhodamine WT and placement of fluorometric devices that detect the concentrations of dye as the dye travels down the aqueduct (see “Dye Study” below). A set of dye and drifters were released simultaneously to capture similar hydrologic conditions. The study was replicated a few hours after the first release by the release of a second set of dye and drifters from the same site as the first release. The dye and drifters were tracked for a period of 7 days along a 75-mile stretch of the aqueduct. Figure 1 illustrates the reach of the study area and the predicted concentrations of the dye.

Many things were learned in the first phase of the study in 2008. For example, it was learned that the stretch of aqueduct being studied should not include a pumping plant so the acoustic tags would survive the trip. To date, only 2 of the 30 deployed tags from both phases have been recovered. The longest stretch of the California Aqueduct without a pumping plant is the stretch after the Dos Amigos Pumping Plant. However, the section immediately after Dos Amigos Pumping Plant was not suitable to deploy tags and dye due to a lack of suitable bridges for deploying the tags and dye. A bridge after Check 14 called O&M Bridge was chosen as the best launch site for the study.

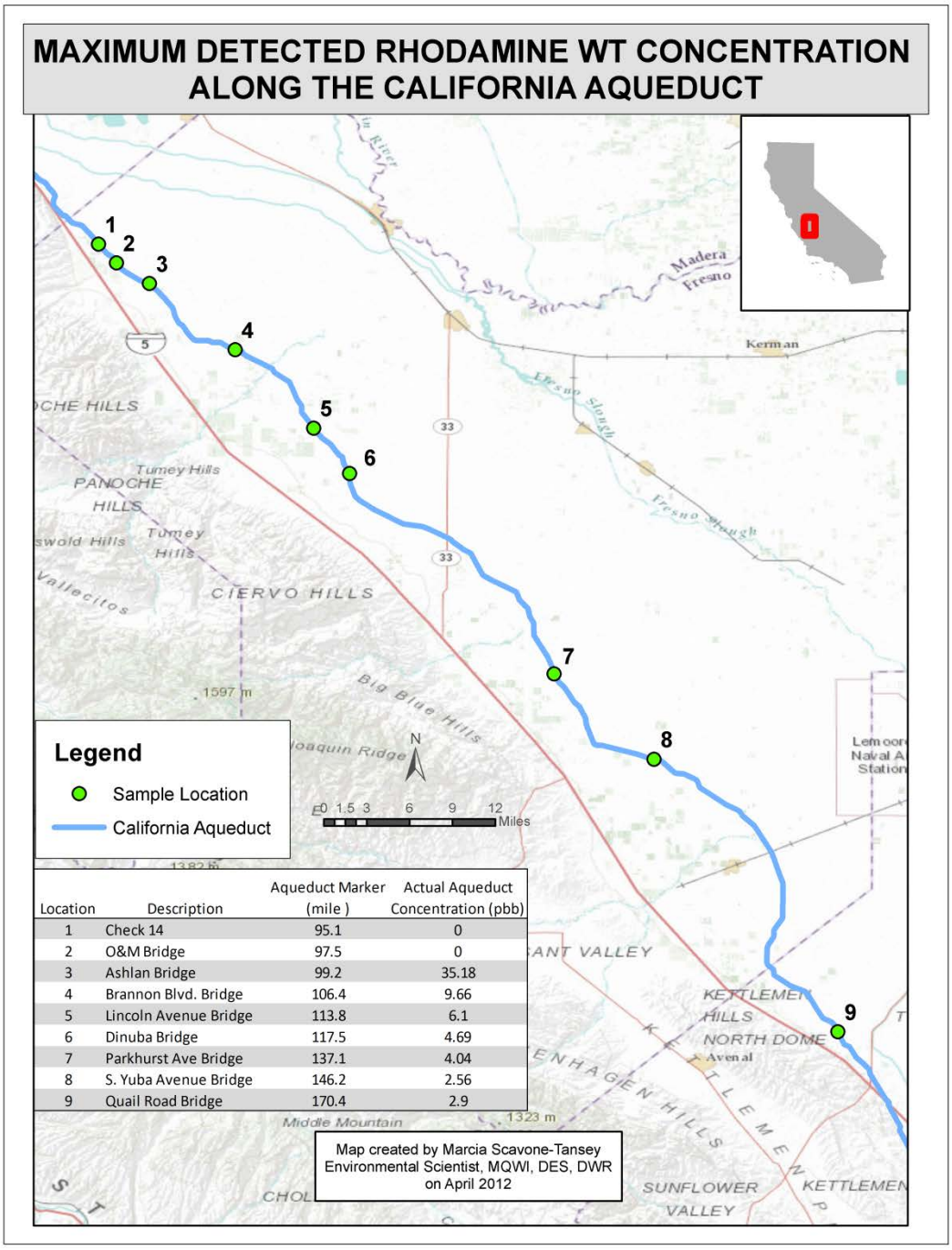

Figure 1: Maximum Detected Dye Concentrations at Study Points within the Study Area

Drifter Study

Photo 1: Neutrally buoyant drifters being manufactured at the MWQI Field Support shop. The orange floats are approximately 2 inches (5 cm) long. The cylindrical black acoustic tags are embedded in the bottom ends of the orange drifters.

The Drifters

The drifters were manufactured from epoxy resin and glass microspheres at the MWQI Field Support Unit shop at the DWR Bryte Laboratory. By adjusting the ratio of epoxy to microspheres, we were able to adjust the density of the float material. This enabled us to produce drifter assemblies that were neutrally buoyant overall.

Each drifter included a commercially manufactured acoustic fish tag designed to emit a high intensity acoustic ping and programmed to ping at intervals that average one minute apart, followed by a sequence of pings that transmit the tag's unique ID code (Vemco, Inc.). Three of the tags also transmitted the depth of their respective drifter. To prevent interference of the fish tags with each other in transmitting their ID signals to the submerged receivers, the tag's internal microprocessor is programmed to produce pings at random intervals between 30 and 90 seconds apart.

Based on lessons learned from the first phase, the density of the epoxy foam portion of the drifters was modified by using less epoxy resin and relatively more glass microspheres. This allows for a smaller drifter design, which it was hoped would minimize entrapment. The first drifters, deployed in August 2008 in the East Branch of the aqueduct, were 7 centimeters at their widest point and had a rounded-edge square box shape. The drifters prepared for the second phase were cylindrical in shape of approximately 5 cm diameter and 6 cm in height, with the negatively buoyant acoustic tag projecting underneath by approximately 1.5 cm. This design change was intended to reduce the probability of entrainment in submerged obstacles and by project trashracks that have a 7.5 cm gap.

The gaps in the trash racks are often partially covered with aquatic macrophytes, which may cause the gap to be less than the design 7.5 cm width. This, in turn, may have interfered with the free movement of drifters of the previous design. As the drifter floated in the water, the transmitting end of the acoustic tags was designed to hang down from one flat end of the drifter cylinder and cause both flat surfaces of the drifter to maintain a horizontal orientation. When the drifters approach a trashrack, they are designed to be properly oriented so that they will pass easily through the vertically oriented slots. However, although one major project trashrack was encountered at Pearblossom Pumping Plant during the first deployment, there were no project trashracks across the aqueduct flow in the second phase study reach. The second

phase study reach does have several turn-outs on the sides of the aqueduct that are protected by trashracks of varying types, sizes, and dimensions.

The Acoustic Receivers

MWQI staff connected the receivers (Vemco VR2R) via Bluetooth to a computer and synchronized each receiver's internal data-logging clock to Greenwich Mean Time (GMT) prior to deployment. As in the first phase of this study, the 10 acoustic receivers were attached to safety ladders on the side of the aqueduct with stainless steel cable and heavy-duty padlocks. The locks were attached near the surface of the water, and the cables put the receivers at a depth of about 3 meters below the water's surface. The safety issues associated with attaching receivers to the side of the aqueduct obligated MWQI staff to prepare a Safety Plan and Job Hazard Assessment. These documents were submitted to the San Luis Field Division Operations Center for approval before the study began. Safety measures observed during receiver deployment and retrieval included use of a five-point harness worn by the person deploying or recovering the receiver, a nylon rope with one end attached to the harness and the other end attached to a vehicle, and a second person standing beyond the aqueduct-sloped side to maintain minimal slack on the rope and to act as an observer.

Previous field tests show that the receivers can detect the tags within the aqueduct at a distance of approximately one kilometer. The receivers were installed along the aqueduct at distances that were at least 3 kilometers apart to prevent overlap of signals. They were also deployed well away from sources of acoustical noise such as aqueduct check structures and obvious turn-out pump locations. Ten locations along the aqueduct were selected near bridges and were also suitable for installing standpipes used for the dye portion of the study. All 10 receivers were installed before the acoustic drifter tags were deployed.

Drifter Deployment Method

The drifters were deployed in two groups of 12 and 13, respectively. The difference in time between group launches depended on the rate of flow at the moment of launch. With the expected amount of dispersion, at least a 4-hour gap was required between groups of drifters. The first group of drifters was launched just before midnight on July 29, 2009; and the second launched around 4 a.m. The drifters were launched by hand from O&M Bridge, milepost 97.5, about 3 kilometers upstream of the first receiver. Three or four transmitting drifters were deployed in each set, and each set was deployed at varying locations across the width of the aqueduct to simulate even lateral distribution. Each set of three or four drifters was deployed with a separation of 2 minutes to lessen the chance of ping interference between drifters. RWT dye was deployed at the same time as the drifters.

Receiver Recovery and Data Collection

The arrival times of the replicate drifter launches at each sampling site were assumed to be similar to the RWT dye arrival times estimated by using a spreadsheet model. The model calculated arrival time of water packets with known flow data measured in cubic feet per second (cfs) and actual channel dimensions at varying aqueduct stages. One day prior to the estimated arrival of the water packet at the study end site, 7 of the receivers that were placed in the first 40 aqueduct miles of the study area (about half the length of the study area) were removed and packed for transport. On the final day of the study, the next two were removed. The largest gap between receivers was 18 miles between the 9th and 10th

receiver. The 10th and final receiver was left in place until 16 days after the RWT dye passed the final receiver to ensure that all drifters had passed by the receiver.

Once the receivers were returned to the MWQI offices, they were scrubbed clean of algae and other organisms that had colonized them during the deployment. The receivers' Bluetooth communication protocols were activated by a magnetic key provided by VEMCO. The acoustic tag binary data collected in the aqueduct were downloaded via Bluetooth connection to a computer running VEMCO software. The data were then exported from the VEMCO software to an Excel spreadsheet for further analyses. The receivers' internal batteries were disconnected to extend their shelf life for potential future use. Finally, the receivers were reassembled with the batteries disconnected and placed in storage at the MWQI office.

Dye Study

Dispersion rates and travel times in aquatic systems vary greatly between systems and even between the reaches of a system (Kilpatrick, 1970). Although approximate ranges of these variables can be estimated from theory, each system must be studied on a case-by-case basis if more precise values are desired. The most common method for calculating time of travel and dispersion rates in a riverine system involves the use of a slug injection of a fluorescent dye into a stream. A slug injection is a single point addition of dye to a stream as opposed to injecting a constant stream of dye over a fixed period of time. Measurements of dye concentration using a fluorometric device are taken downstream from the injection site after the dye has traveled a sufficient distance to be fully mixed across the channel vertically and horizontally. The fluorometric devices used to measure the concentrations along the aqueduct were Turner Designs SCUFAs. SCUFA is a product name that stands for Self Contained Underwater Fluorometric Apparatus. These fluorometric devices are factory-configured for the fluorescent wavelength of RWT and also able to independently detect and record turbidity. Concentration measurements are then taken at several distances farther downstream of the initial sampling site. The differences in concentrations and length of the dye pulse observed at each site are used to calculate the time of travel and the dispersion rate of the system. As previously described, RWT dye releases were made at the same time as the drifters were deployed.

Rhodamine WT

Preparations before Study

Rhodamine WT (RWT) is the only fluorescent dye approved by the U.S. Food and Drug Administration (FDA) and the U.S. Environmental Protection Agency (EPA) for use as a tracer in drinking water systems (FDA, 1966 and EPA, 1998). EPA suggests that if the standards for RWT use—which are set forth by the National Sanitation Foundation (NSF)—are met, water treated with RWT is safe for human consumption (NSF International 2003). The NSF standards allow for RWT concentrations of up to 10 parts per billion (ppb) at the intake of a drinking water treatment plant. Kilpatrick of the USGS developed general formulas for estimating the concentration of RWT at a site downstream of a slug injection. These formulas are based on multiple empirical studies of different streams and can be applied to any aquatic fluvial system to ensure proper dosage of dye. MWQI staff used the following formula to calculate the concentration needed:

$$V_S = 3.4x10^{-4} (Q_m L/\nu)^{0.94} C_P \qquad \text{Equation 1}$$

Where:
V_S = volume of stock Rhodamine WT 20% dye, in liters
Q_m = maximum stream discharge at the downstream site, in cfs
ν = stream velocity, in feet per second (ft/s)
C_P = peak concentration at the downstream sampling site, in micrograms per liter (ppb)
L = distance to the downstream site, in feet

The previous formula was solved for C_P to estimate what the concentration at downstream locations would be following the slug injections as follows:

$$C_P = V_S/3.4x10^{-4} (Q_mL/\nu)^{0.94} \quad \text{Equation 2}$$

During the field study, DWR Field Division aqueduct system operators were consulted by phone to determine Q_m, the water discharge flowing past each check structure. The aqueduct is a designed system that has known dimensions of maximum depth, width across the channel bottom, and side slopes. Stream velocity (ν) was calculated based on known channel dimensions and the discharge in cfs using the following formula;

$$\nu = Q_m/A \quad \text{Equation 3}$$

Where:
A= area of cross section of the channel (in square feet).

When the stream velocity is calculated in this manner, stream discharge (Q_m) is found in both the numerator and denominator and the equation can be simplified to:

$$V_S = 3.4x10^{-4} (Q_mL/\nu)^{0.94} C_P \quad \text{Equation 4}$$

$$V_S = 3.4x10^{-4} (Q_mL/ Q_m/A)^{0.94} C_P \quad \text{Equation 5}$$

$$V_S = 3.4x10^{-4} (LA)^{0.94} C_P \quad \text{Equation 6}$$

This simplification of Kilpatrick's formula can be made because the aqueduct is a trapezoidal channel and maintains essentially the same cross sectional area throughout each pool except for short reaches near check structures. For our purposes, these short reaches are assumed to not significantly affect the estimate.

Water in the aqueduct carries suspended particles, such as algae and silt, that scatter light (turbidity). These particles may cause false RWT concentration readings in the SCUFAs as they flow through the sensors at the sample sites. Several apparent outliers were observed in the raw data. To remove these outliers, a locally weighted scatterplot smoothing (lowess) operation was performed on the unmodified RWT concentration data, and the time data using a 10% smoothing factor (Minitab 14 statistical software). The fits and residuals of this lowess smooth are saved for further analysis (Figures 2 through 4). The fitted line is smooth and represents a localized best fit through the data points. The lowess residual data was then modified in Microsoft Excel by taking its absolute value and removing the 10% of the data points farthest from the smoothing line. In this way, 90% of the data remained, and the data maintained the same shape while the data most likely to be erroneous outliers were removed. Figure 2 shows an example of the raw RWT concentration data plotted over time at the Brannon Bridge site. Figure 3 shows the same data after the outliers have been removed. Decimal dates were used to represent time in the analysis of this data. For reference, 40024.50 is July 30, 2009, at 1200 hours. The SCUFAs sampled RWT concentration and turbidity at one-minute intervals.

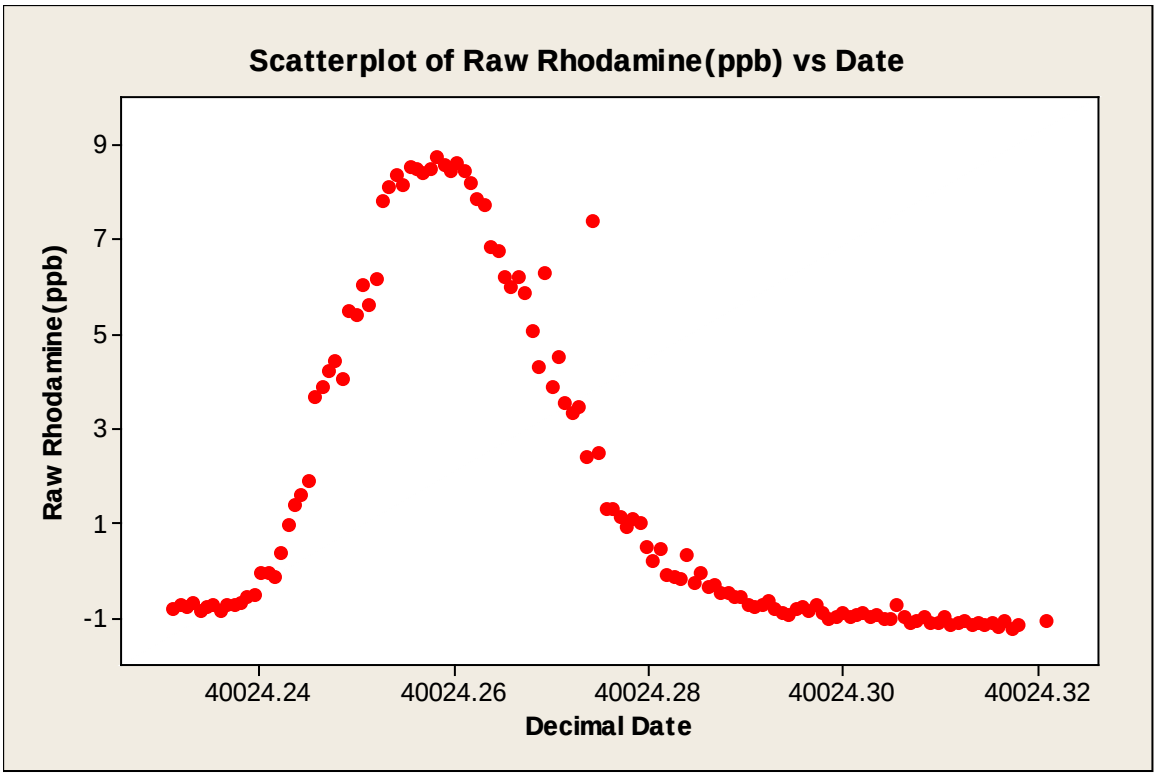

Figure 2: Scatterplot of Raw Data from the SCUFA as RWT Dye Pulse 1 Passed by Brannon Bridge, Milepost 106.4

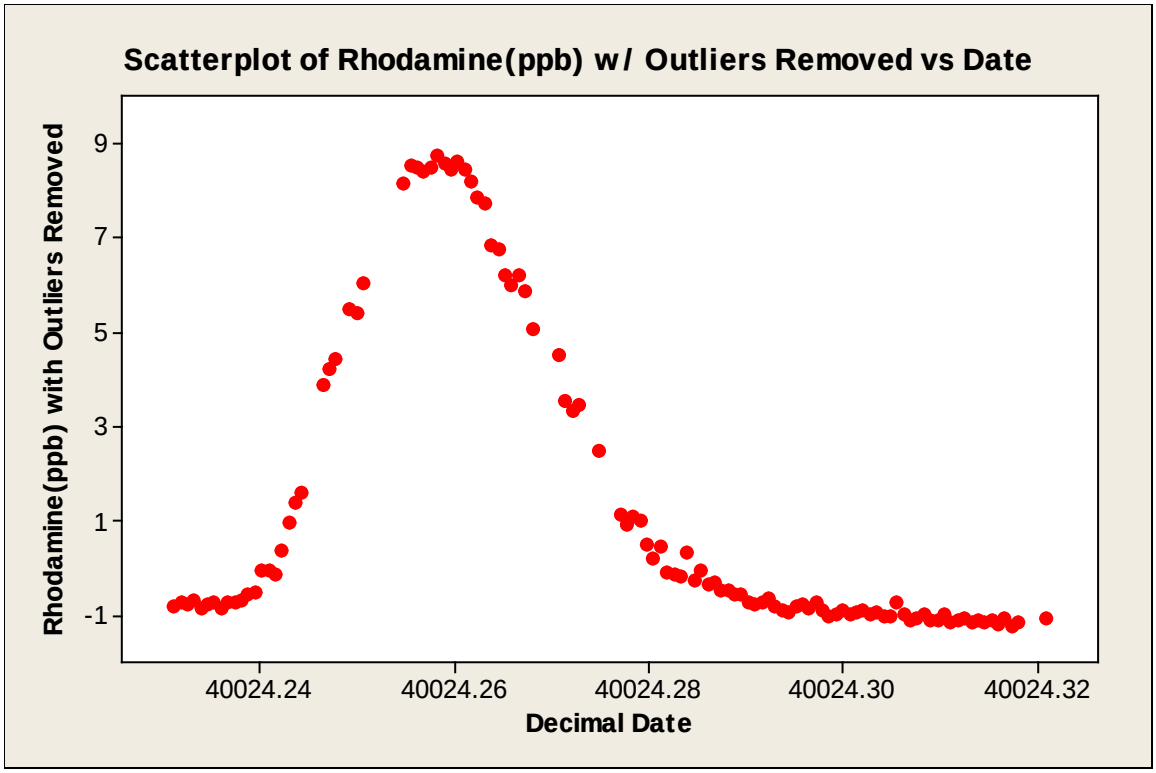

Figure 3: Scatterplot of Data with Outliers Removed (same event as Figure 2)

When deciding what portion of data was to be considered outliers, it was discovered that when less than 10% was removed from some concentrations, curves still contained data points that were obvious outliers. The 10% rule was applied consistently across all curves because it removed the minimum amount of RWT concentration data points, yet ensured that all extraneous data were removed from each RWT concentration data set at each sampling location. In some curves, up to 2% additional non-extraneous data were removed.

A smooth curve was made through the data sans outliers using a lowess smoothing. This smooth curve eases the calculations for creating a model of the RWT concentration data based on the Gaussian distribution. Figure 4 is an example of the lowess-smoothed data. The lowess smoothing factor was 10%.

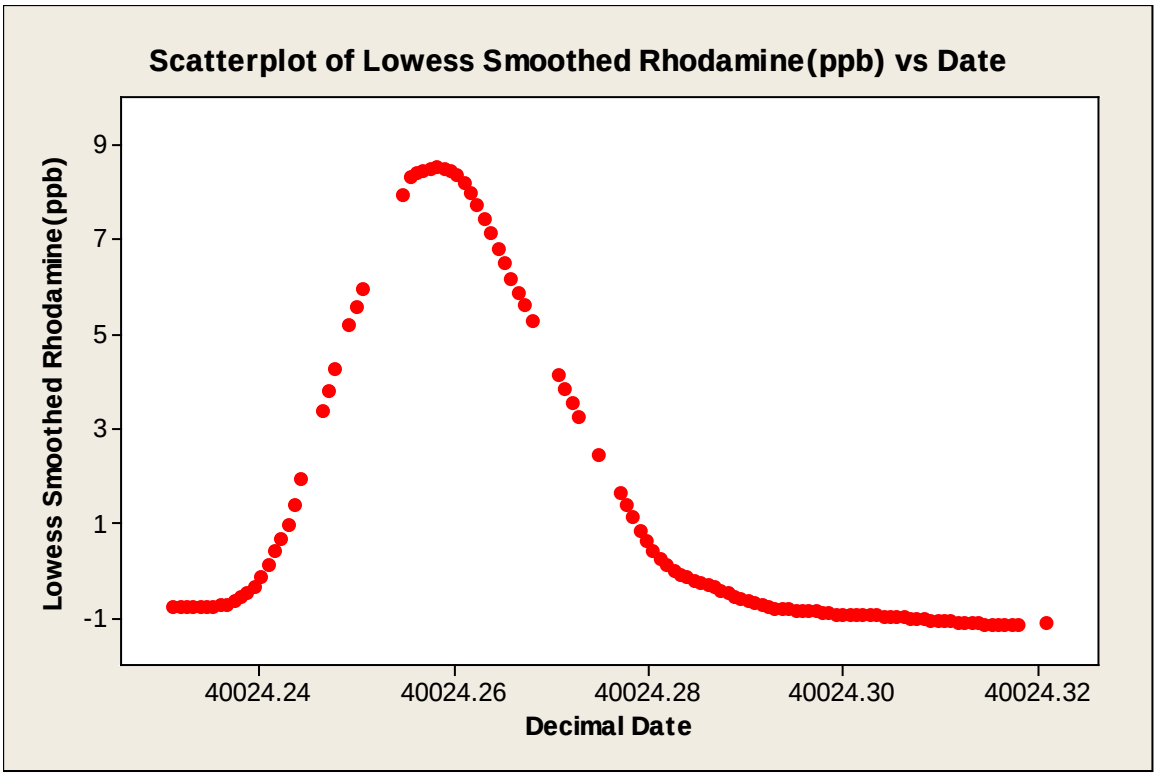

Figure 4: Scatterplot of Fitted RWT Concentration Data over Time (same event as Figure 2)

Background Fluorescence Due To Other Suspended Matter

Water in the aqueduct carries suspended particles that give each sample site its own unique background fluorescence at the same wavelength as RWT. This changes the RWT concentrations detected by the SCUFA sensors, which vary among measurement sites. The background fluorescence was removed from the outlier-free RWT concentration data by subtracting the value of the lowest RWT concentration detected in the sample period at each site from all the concentrations in that period. The baseline RWT concentration at each site was set to zero through this method, which makes possible comparisons of the concentration curves. Figure 5 shows the baseline-corrected data for RWT concentration pulse #1 at Brannon Bridge.

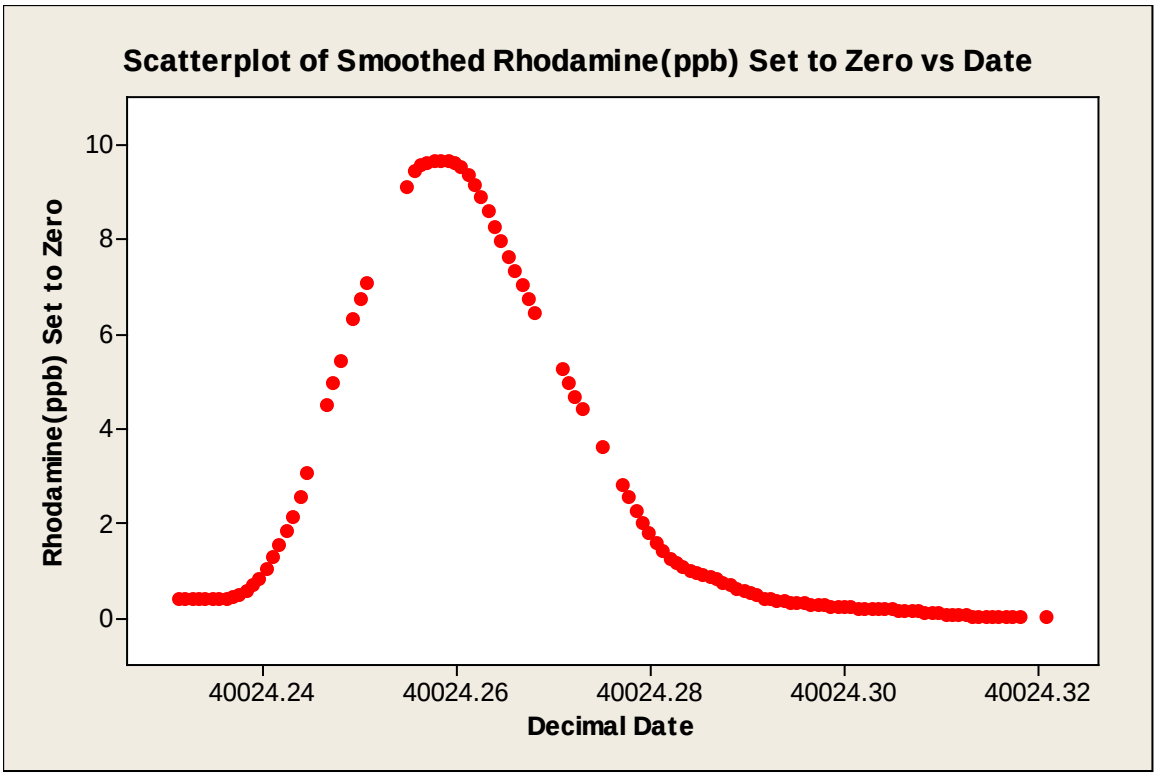

Figure 5: Scatterplot of Data from Figure 4 with Background Offset Removed

The corrected RWT concentration data provide smooth curves for each dye pulse event that are comparable for further analysis. Each curve appears similar to a Gaussian or bell-shaped curve, as theory predicts (e.g., Fischer *et al*., 1979). This is useful for data-fitting purposes because the formula for a Gaussian is straight-forward and commonly available in statistical software. It is as follows:

$$f(x) = ae^{-\frac{(x-b)^2}{2c^2}}$$ Equation 7

Where:

f(x) = the concentration of the constituent of interest (in this case, RWT);
x = the time variable;
a = the maximum concentration at the peak;
b = the time of maximum peak;
c = (FDHM)/($2\sqrt{2\ln 2}$)

The c term in this equation is found by first determining the full duration at half maximum (FDHM). FDHM is defined as the time difference between the two points on either side of the curve where the RWT concentration is half the value of the peak or maximum RWT concentration. Secondly, the FDHM is divided by $2\sqrt{2\ln 2}$ to get c. The c term is comparable to the standard deviation or σ found in a Gaussian where the area under the curve is fixed at one.

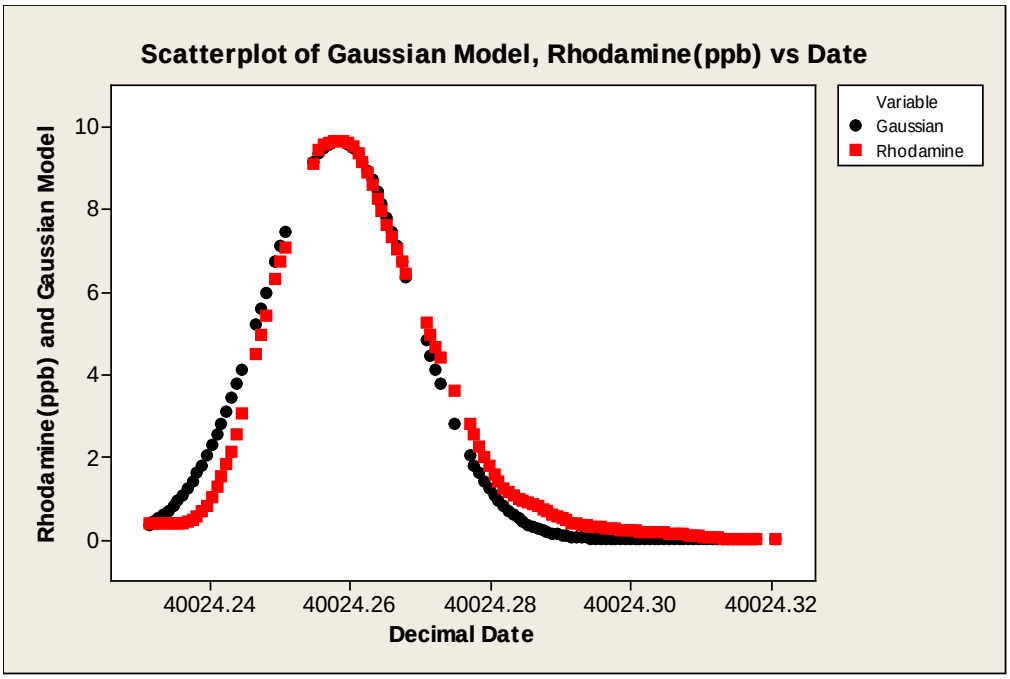

Figure 6: Scatterplot of Data from Figure 5 with Gaussian Model Superimposed for Comparison

Figure 6 illustrates a Gaussian distribution that has the same peak height and width at half height with the lowess smoothed data from Figure 5.

The Gaussian models were compared to the adjusted RWT (ppb) data using a Pearson's Correlation test to determine the goodness of fit. As an example, Table 1 summarizes the statistical analysis of the graphical data presented in Figure 6.

The example in Table 1 shows the Pearson's Correlation value or Pearson's r of 0.989 indicating that the modeled data explain 98.9% of the variation in the observed data. The Pearson's Correlation P value of 0.000 indicates that there is less than 0.05% chance that this result was random. The analyses were done with a 95% two-sided confidence interval.

Table 1: Example of Statistical Analyses of Modeled and Adjusted RWT Concentration Data from Brannon Bridge Pulse 1

Site and RWT pulse	Pearson's Correlation or r	Correlation P-Value
Brannon Pulse 1	0.989	0.000

To calculate the absolute rates of dispersion of a dye plume, the following information is required from the RWT dye curves:

C_p	=	peak concentration of dye plume
T_l	=	arrival time of dye plume leading edge, defined as time at which RWT concentration was 0.1% of C_p
T_p	=	arrival time of dye plume peak concentration
T_{10p}	=	arrival time of dye plume trailing edge, where dye concentration has fallen to 10% of the peak concentration
T_t	=	arrival time of dye plume trailing edge, defined as time at which RWT concentration of 0.1% of C_p

Figure 7 illustrates the data requirements.

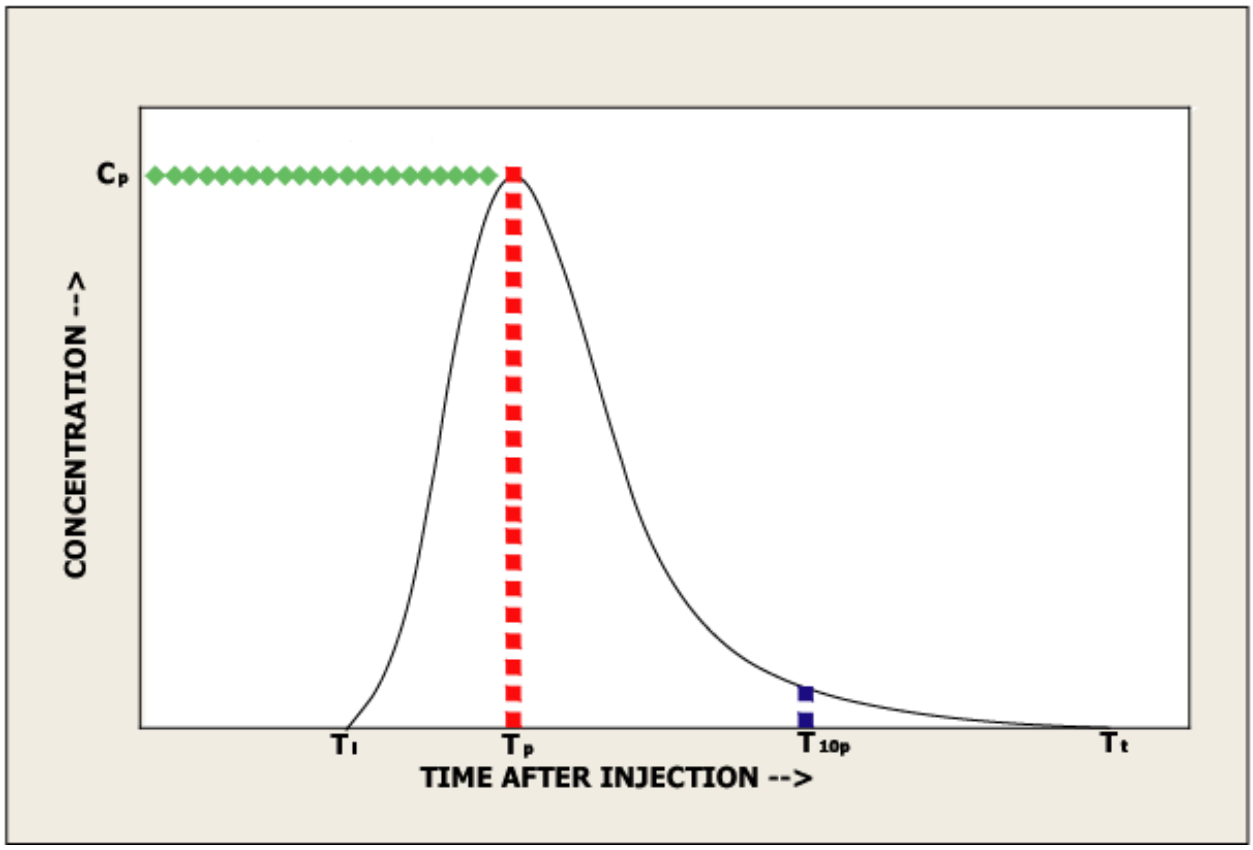

Modified from Kilpatrick and Wilson, 1989

Figure 7: Typical Time-concentration Curve for Movement of Dye Past Fixed Measurement Point downstream from Dye Injection

The mean travel time (t_p) for a RWT plume between two locations is the difference in elapsed time between the RWT concentration peaks at the two locations:

$$t_p = T_{p(n+1)} - T_{p(n)} \quad \text{Equation 8}$$

Where (n) denotes one data point and ($n+1$) being the next data point.

The travel time of the leading edge of each RWT plume (t_l) is calculated as:

$$t_l = T_{l(n+1)} - T_{l(n)} \quad \text{Equation 9}$$

The travel time of each peak concentration (t_p) of is calculated similarly:

$$t_p = T_{p(n+1)} - T_{p(n)} \quad \text{Equation 10}$$

Note that the mean travel (t_p) for a RWT concentration plume is the same as the travel time of the peak (t_p). This is because the peak is at the exact middle of the Gaussian model by design.

The travel time of the trailing 10% of peak (t_{10d}) is by:

$$t_{10p} = T_{10p(n+1)} - T_{10p(n)} \quad \text{Equation 11}$$

The travel time of each trailing edge (t_t) is calculated by:

$$t_t = T_{t(n+1)} - T_{t(n)} \quad \text{Equation 12}$$

These travel times are used to calculate the mean sheer velocity of the RWT plume as it passes through each reach of the aqueduct (defined or bounded by two fluorometric observation sites). The mean sheer velocity is the average velocity of each plume calculated using the travel times of the leading edge, peak, and trailing edge points on each curve. The following general formula was used:

$$\frac{D_{A(n-1)} - D_{A(n)}}{t} = V \quad \text{Equation 13}$$

Where:

t	= respective arrival times derived from the previous formulae
$D_{A(n)}$	= aqueduct mile where SCUFA device was placed.
$D_{A(n-1)}$	= mile upstream of where previous SCUFA was placed, or RWT deployment site
$V_{tl, tp, t10p, \text{ and } tt}$	= mean sheer velocity of RWT plume at select travel times, t_l, t_p, t_{10p}, and t_t.

These velocities at travel times t_l, t_p, and t_t are averaged to get a mean velocity of the entire plume V_{plume}. This number is very close to the velocity calculated at t_p.

The length of the plume, l_{plume} as it passes a sampling site was calculated by:

$$V_{plume}(t_t - t_l) = l_{plume} \quad \text{Equation 14}$$

Knowing the length of the plume in feet permits the calculation of the rate each plume dispersed longitudinally with the following formula:

$$K_d = \frac{l_{plume(n+1)} - l_{plume(n)}}{t_t}$$ Equation 15

K_d = rate of dispersion

Rates of dispersion were calculated for each stretch of water between sampling sites.

Equipment and Personnel Used

Both the first and second phases of the study had many aspects that required the knowledge and expertise of a diverse group of DWR staff. MWQI staff acquired the necessary equipment for this study from various suppliers and in some cases manufactured elements at DWR facilities. Table 2 summarizes the equipment and personnel needed to implement the second phase of this study.

Table 2: Resource Requirements for Dye Study

Staff required	
For the field portion:	Hours used
One MWQI environmental scientist	120 hours
One MWQI staff environmental scientist	80 hours
One MWQI field support environmental scientist	120 hours
One San Luis Field Division water quality technician	80 hours
For the shop portion:	
Two MWQI environmental scientists	140 hours
One MWQI staff environmental scientist	60 hours
Three MWQI field support environmental scientists	200 hours
One MWQI field support student	16 hours
Equipment required	Vendor acquired from
Three Turner Designs SCUFAs	Rented from Orders Associates Research Systems
30 liters of Rhodamine dye	Purchased from Organic Dyestuffs Corporation
Standpipes	Fabricated by MWQI Field Support Staff
Vehicles required	Time needed
MWQI field truck with rack and tool chests	12 days
DES Taurus pool vehicle	5 days

Placement of the SCUFAs into the aqueduct involved designing and building temporary movable standpipes to hold the fluorometric devices and their floats and identifying suitable bridges on which to mount the standpipes. This involved both MWQI office and field staff for fabrication of standpipes and the standpipe fasteners required to hold the SCUFAs in place. It also involved the San Luis Field Division to help identify all possible municipal water turn-outs so that all affected parties could be contacted. Several reconnaissance trips were required to identify the bridges used to mount SCUFA standpipes and to determine the engineering required for secure standpipe stabilization. Seven MWQI staff members were required to conduct this study. Table 3 outlines the deployment schedule of equipment.

Table 3: SCUFA Deployment Times

Bridge	Mile marker	SCUFA #	Tuesday July 28	Thursday July 30	Friday July 31	Saturday August 1	Sunday August 2	Monday August 3
Ashlan	99.2	1	Installed 21:45	Removed 07:30				
Brannon	106.4	2	Installed 22:15	Removed 13:30				
Lincoln	113.8	3	Installed 23:00	Removed 20:00				
Dinuba	118.5	1		Installed 09:30				
Dinuba	*118.5*	*1*		Removed 23:30				
San Diego	121.8	2		Installed 14:30				
San Diego	*121.8*	*2*		Removed 24:00				
San Mateo	130.8	3		Installed 21:00		Removed 13:00		
Parkhurst	137.1	1			Installed 00:30		Removed 09:00	
Yuba	146.2	2			Installed 01:30		Removed 11:00	
Quail	167.4	3				Installed 14:00		Removed 10:00

Analysis

The two simultaneous studies (within phase 2) involving both drifters and dye release required different procedures for analysis. Upon reviewing the data of each study the investigators decided not to fully analyze both studies. It became clear that one of the studies did not answer the questions that the studies set out to answer.

Drifter Study

The phase 1 drifter study during summer 2008 in the East Branch of the California Aqueduct proved that neutrally buoyant drifters with embedded acoustic tags can be tracked as they travel along a concrete-lined trapezoidal channel, and that travel time and dispersion rate were measurable. However, the data collected during phase 1 raised the concern that the drifters may not behave the same as a dissolved constituent in flowing water. The dye study was intended to determine whether or not the neutrally buoyant drifters move faithfully with water particles.

In the 2009 study (Phase 2), the observational data from the acoustic receivers showed that only 12 of the 25 drifters arrived at the final receiver located at the Quail Bridge sampling site by the time the receiver was removed on August 18, 2009. The rest of the drifters were either entangled in the aqueduct or diverted at one of the many turn-outs. One drifter was spotted and retrieved from an algal mass on the side of the aqueduct on August 1 (Photo 1). The first drifter arrived at Quail Bridge at 19:19 August 3, 2009, but the first pulse of RWT arrived at the same site two days earlier at 19:12 on August 1. The second pulse of RWT had completely passed Quail Bridge by the morning of August 2, and no drifters had arrived at the sampling site at that time. The last drifter was detected at Quail Bridge at 09:24 August 14—a full 12 days after the last dye pulse had passed by.

Based on this initial data the investigators determined that the drifters do not accurately reflect water movement, and it was not necessary to further analyze the drifter data. Figure 8 shows the concentration curves of the two pulses of RWT passing Quail Bridge in black and red and the detections of drifters passing the same site in green. The two deployments of drifters were completely merged and indistinguishable by the time they reached the final receiver at Quail Bridge.

Photo 2: A drifter found entangled in a mass of algae on the side of the aqueduct. This drifter was recovered thanks to the sharp eyes of one of the investigators. The drifter is approximately 2 inches (5 cm) long. The cylindrical black acoustic tag is embedded in the bottom end of the drifter (not visible).

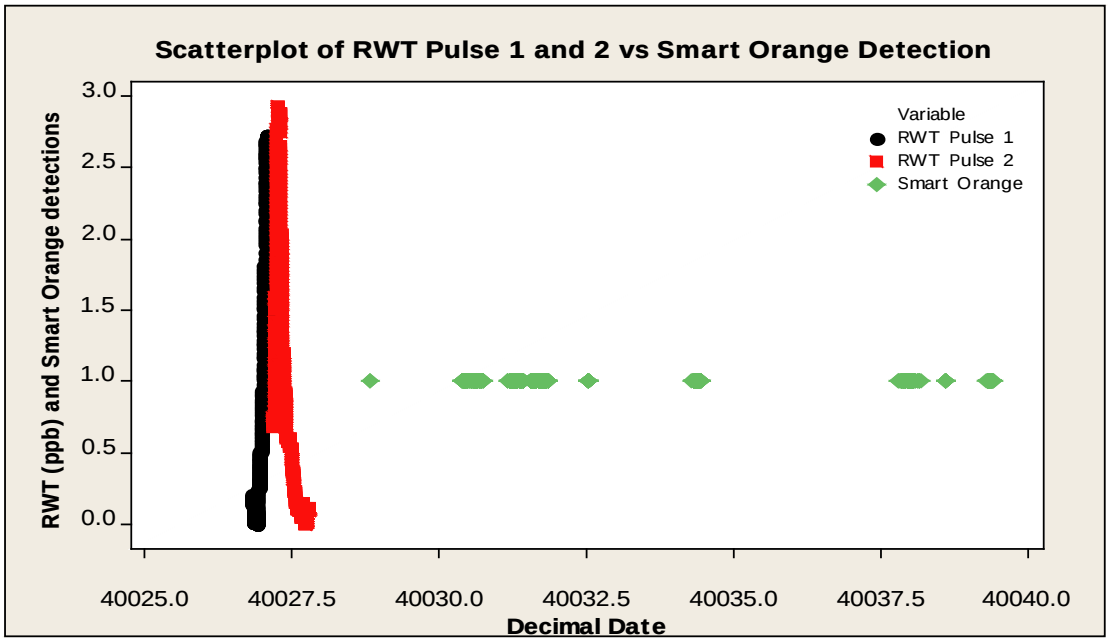

Figure 8: Scatterplot of Both Pulses of RWT (ppb) and 'Drifter' Detections at Quail Bridge

Dye Study

The dye study proved better at resolving the study questions than the drifter study. For example, a reasonable assumption can be made that the dye behaved similarly to the water in the aqueduct. The fast sampling rates in the SCUFA fluorometers provided detailed data that enabled us to discern subtle features of the waterflow. The study highlights the unique properties of the aqueduct that make it different than a typical riverine fluvial system. A trapezoidal, concrete-lined canal of known dimensions should, in theory at least, make much of the data analysis simple. However, the complex way the aqueduct is managed created additional unexpected effects.

Most river systems have a complex channel morphology where many factors vary along its reach. Channel depth, width, and shape vary and affect how water moves in a riverine system. Flow in a river tends to be conserved in the absence of water diversions. The aqueduct is managed to take advantage of energy prices that fluctuate during a 24-hour daily cycle. Water is pumped more during the night when electricity is least expensive, and flows can approach the aqueduct's maximum flow capacity during this period. (The aqueduct portion used in this study has a maximum flow capacity of 13,800 cfs; other portions are generally less.) When the energy cost increases during the day, flows in the aqueduct can be reduced to its minimum gravity-driven flow of 3 to 5 cfs, according to O&M staff.

There are many sites along the aqueduct where water is diverted from or pumped into the canal. The investigators observed periods when the flow of the aqueduct was reversed as water was diverted for agricultural use upstream of sampling sites. A river's flow is relatively constant and does not reverse in direction under normal circumstances. This reverse flow is common enough an event that it was apparently observed in the data collected at one of the sampling sites for the dye study. This is discussed in more detail below.

Dye Plume Curves

Recall that two dye releases were made at O&M Bridge. Unfortunately, we were not able to capture both RWT plumes at all the sampling sites due to time restrictions during the study. The three SCUFAS were leapfrogged down the California Aqueduct based on estimated arrival times of the dye plumes. The estimates were based on a particular flow rate. Unfortunately the rate of flow was at times much faster or slower than anticipated and the SCUFAs were moved too soon or arrived too late to catch a particular pulse The sites where RWT dye peak data were captured are Ashlan, Brannon, Lincoln, Dinuba, Parkhurst, Yuba, and Quail bridges for RWT plume 1. For RWT plume 2, data were collected at Ashlan, Brannon, Parkhurst, and Quail bridges.

The first analysis of the collected data involved creating Gaussian curve models that best fit the data. The appendix includes scatterplots of the raw RWT concentration data, the smoothed and zeroed RWT concentration data, and the Gaussian model of the data at each site. The models were shifted along the x-axis (time) to best match observed data as determined by Pearson's correlation test for paired data. Table 4 shows how the Gaussian models match the observed RWT (ppb) data very well.

Table 4: Pearson Correlations of Modeled and Fitted Rhodamine Data

Site and RWT pulse	Pearson Correlation (rho)	P-Value
Ashlan Bridge Pulse 1	0.904	0.000
Brannon Bridge Pulse 1	0.989	0.000
Lincoln Bridge Pulse 1	0.971	0.000
Dinuba Bridge Pulse 1	0.997	0.000
Parkhurst Bridge Pulse 1 *	0.783	0.000
Yuba Bridge Pulse 1	0.999	0.000
Quail Bridge Pulse 1	0.985	0.000
Ashlan Bridge Pulse 2	0.975	0.000
Brannon Bridge Pulse 2	0.978	0.000
Parkhurst Bridge Pulse 2	0.998	0.000
Quail Bridge Pulse 2	0.971	0.000

*The low correlation value found for Parkhurst Bridge Pulse 1 is due to flow anomalies that are discussed in this section.

Figure 9 and Figure 10 are scatterplots of the Gaussian models created to analyze the dye behavior of RWT pulses 1 and 2. The graphs show a decrease in the peak Rhodamine concentrations over time, as is expected from the dispersion equation(Equation 15). The curves also show a lengthening at the base of the plumes as the RWT dispersed longitudinally.

The distances between the RWT launch site and each sampling site are listed in Table 5.

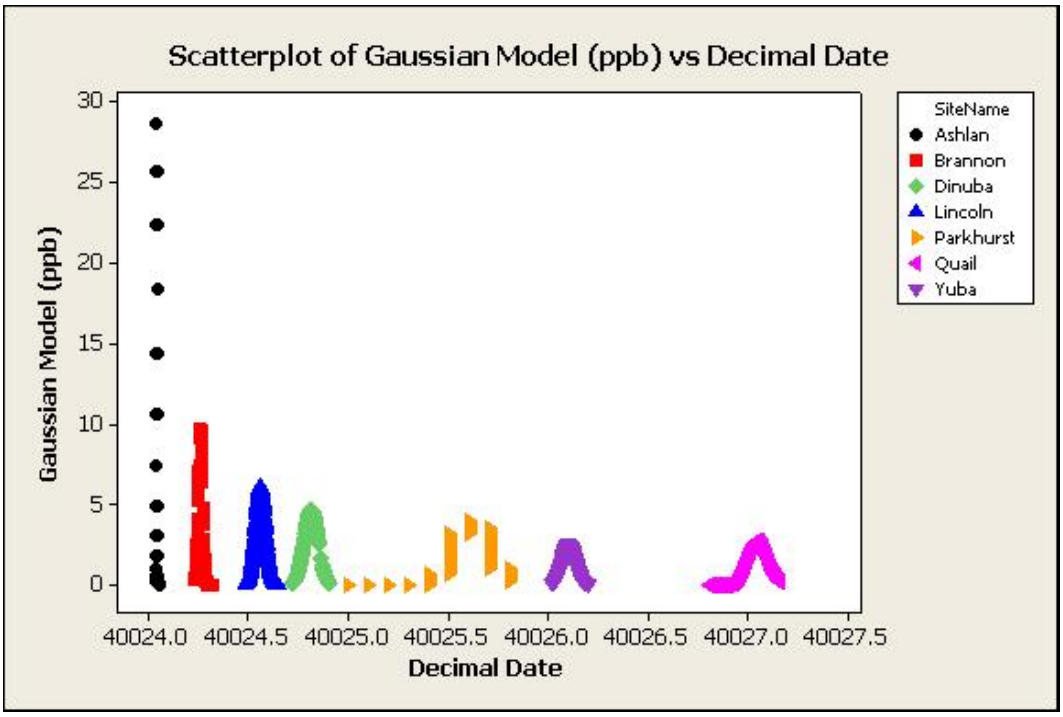

Decimal Date 40024 Corresponds to July 30, 2009

Figure 9: Scatterplot of Gaussian Models at Each Sample Site over Time for RWT Pulse 1

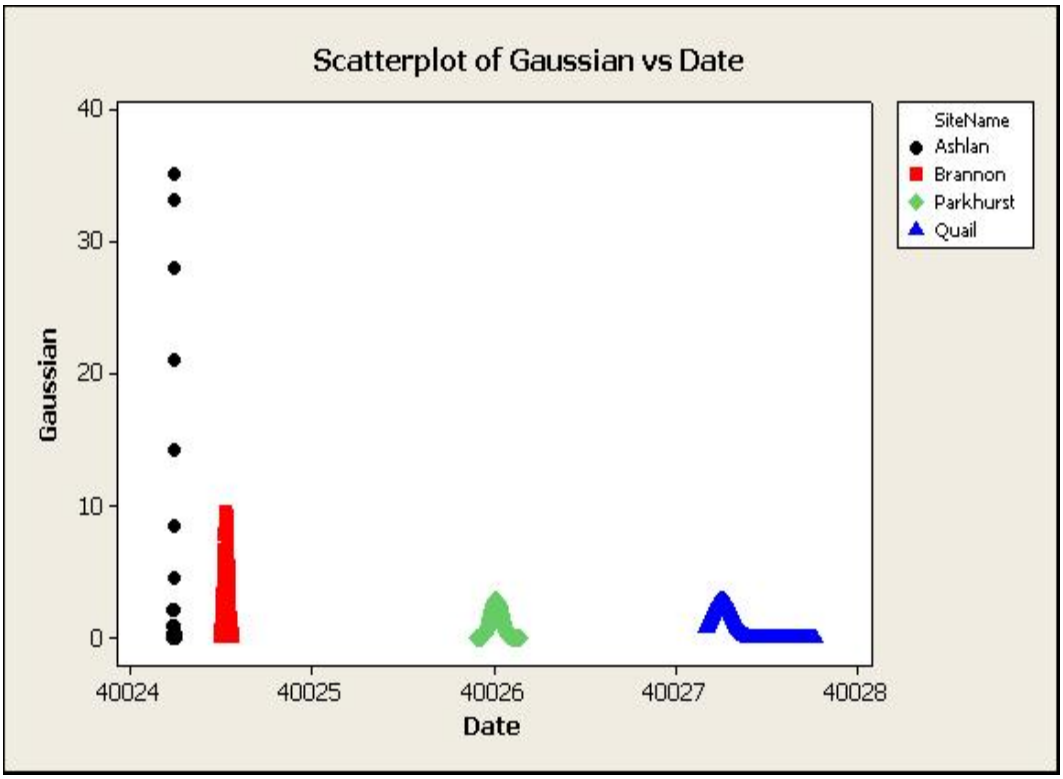

Date 40024 corresponds to 30 July 2009.

Figure 10: Scatterplot of Gaussian Models at Each Sample Site over Time for RWT Pulse 2

Table 5: Distance in Miles between Each Reach of the Study

Distance in miles	Ashlan	Brannon	Lincoln	Dinuba	Parkhurst	Yuba	Quail
Distance From O&M	1.7	8.9	16.3	21	39.6	48.7	69.9
Distance From Ashlan		7.2	14.6	19.3	37.9	47	68.2
Distance From Brannon			7.4	12.1	30.7	39.8	61
Distance From Lincoln				4.7	23.3	32.4	53.6
Distance From Dinuba					18.6	27.7	48.9
Distance From Parkhurst						9.1	30.3
Distance From Yuba							21.2

The first RWT sampling location, Ashlan Bridge, was 1.7 miles downstream from the RWT deployment site at O&M Bridge. The final sampling location, Quail Bridge, was 69.9 miles downstream from the RWT deployment site. The largest distance between two sequential sampling locations was between Yuba Bridge and Quail Bridge, which are 21.2 stream miles apart.

The times of travel (t) shown in Tables 6 and 7 represent the amount of time in decimal days it took for each point (leading edge, peak, 10% of peak and trailing edge) of the RWT plume to arrive at the sampling location. RWT plumes 1 and 2 arrived at the first sampling site about 1.27 hours and 1.35 hours, respectively, after the release time at O&M Bridge. RWT plumes 1 and 2 arrived at the final sampling site about 69.24 hours and 68.81 hours after their respective release time.

Table 6: Travel Times for Leading Edge (t_l), Peak (t_p), 10% of Peak (t_{10p}), and Trailing Edge (t_t) of RWT Pulse 1, in Days (1.00 = 24 hours)

Time in days	Ashlan	Brannon	Lincoln	Dinuba	Parkhurst	Yuba	Quail
t_l from O&M	0.052939	0.243190	0.493169	0.707181	1.315575	1.999358	2.884904
t_p from O&M	0.063900	0.282650	0.581956	0.835428	1.631262	2.124317	3.070150
t_{p10} from O&M	0.070229	0.305433	0.633217	0.909472	1.813523	2.196462	3.177103
t_t from O&M	0.074862	0.322111	0.670743	0.963676	1.946948	2.249276	3.255397
t_l from Ashlan		0.190251	0.440230	0.654242	1.262636	1.946419	2.831965
t_p from Ashlan		0.218750	0.518056	0.771528	1.567361	2.060417	3.006250
t_{p10} from Ashlan		0.235204	0.562988	0.839243	1.743294	2.126233	3.106874
t_t from Ashlan		0.247249	0.595881	0.888814	1.872086	2.174414	3.180535
t_l from Brannon			0.249980	0.463991	1.072386	1.756168	2.641714
t_p from Brannon			0.299306	0.552778	1.348611	1.841667	2.787500
t_{p10} from Brannon			0.327784	0.604039	1.508090	1.891029	2.871669
t_t from Brannon			0.348632	0.611289	1.624837	1.927165	2.933286
t_l from Lincoln				0.214011	0.822406	1.506189	2.391735
t_p from Lincoln				0.253472	1.049306	1.542361	2.488194
t_{p10} from Lincoln				0.276255	1.180306	1.563245	2.543885
t_t from Lincoln				0.262658	1.276205	1.578534	2.584654
t_l from Dinuba					0.608395	1.292177	2.177723
t_p from Dinuba					0.795833	1.288889	2.234722
t_{p10} from Dinuba					0.904051	1.286990	2.267631
t_t from Dinuba					1.013547	1.315876	2.321997
t_l from Parkhurst						0.683783	1.569329
t_p from Parkhurst						0.493056	1.438889
t_{p10} from Parkhurst						0.382939	1.363579
t_t from Parkhurst						0.302328	1.308449
t_l from Yuba							0.885546
t_p from Yuba							0.945833
t_{p10} from Yuba							0.980640
t_t from Yuba							1.006121

Table 7: Travel Times for Leading Edge (t_l), Peak (t_p), 10% of Peak (t_{10p}), and Trailing Edge (t_t) of RWT Pulse 2, in Days (1.00 = 24 hours)

Time in days	Ashlan	Brannon	Parkhurst	Quail
t_l from O&M	0.056228	0.303280	1.723623	2.867291
t_p from O&M	0.063900	0.349317	1.835428	3.064595
t_{p10} from O&M	0.068330	0.375897	1.899979	3.178508
t_t from O&M	0.071573	0.395355	1.947234	3.261899
t_l from Ashlan		0.247052	1.667395	2.811063
t_p from Ashlan		0.285417	1.771528	3.000694
t_{p10} from Ashlan		0.307567	1.831649	3.110178
t_t from Ashlan		0.323781	1.875660	3.190325
t_l from Brannon			1.420343	2.564011
t_p from Brannon			1.486111	2.715278
t_{p10} from Brannon			1.524082	2.802611
t_t from Brannon			1.551879	2.866544
t_l from Parkhurst				1.143668
t_p from Parkhurst				1.229167
t_{p10} from Parkhurst				1.278529
t_t from Parkhurst				1.314665

The two pulses remained distinguishable throughout the study period. At the final sampling site, the pulses overlapped for about 4.5 hours, but could still be fully resolved. Also at the final sampling site the RWT pulses 1 and 2 were 8.89 and 9.47 hours long, respectively. During the overlapped time, each pulse was at or below approximately 10% of its peak concentration. The influence of one pulse had little effect on the modeled curve of the other. After subtracting the influence of one pulse from the other, the fitted peak of each pulse was lowered by about 0.002 ppb, which is well below the 0.05 ppb detection limit of our instruments. The other parameter used to create models for each peak was the full width at half peak height of the measured fluorescence data. At this point, the difference between the raw data and the data with each curve's influence subtracted was about 0.01 ppb, which is also below the detection limit of 0.05 ppb of the equipment.

Figure 11 is a scatterplot of RWT pulse 1 and 2 data in blue and red, respectively, from the Quail Bridge sampling site. The purple data in Figure 11 are the result of subtracting pulse 2 from pulse 1. The green data in Figure 11 are created by subtracting pulse 1 from pulse 2. The y-axis of this graph is RWT in ppb, and the x-axis is the sequence position in time of each RWT measurement. The subtractions were to eliminate the influence of the one pulse over the other. The zero position was chosen arbitrarily prior to the beginning of the pulse. The final position is 900 minutes after the arbitrary beginning.

Graphically, the point where each plume had the largest influence on one another was around sample 440 where the red and blue plots intersected. Because the two RWT plumes did not influence the modeled data by a factor greater than our equipments precision, the models were not changed at this sampling site to reflect that minor influence.

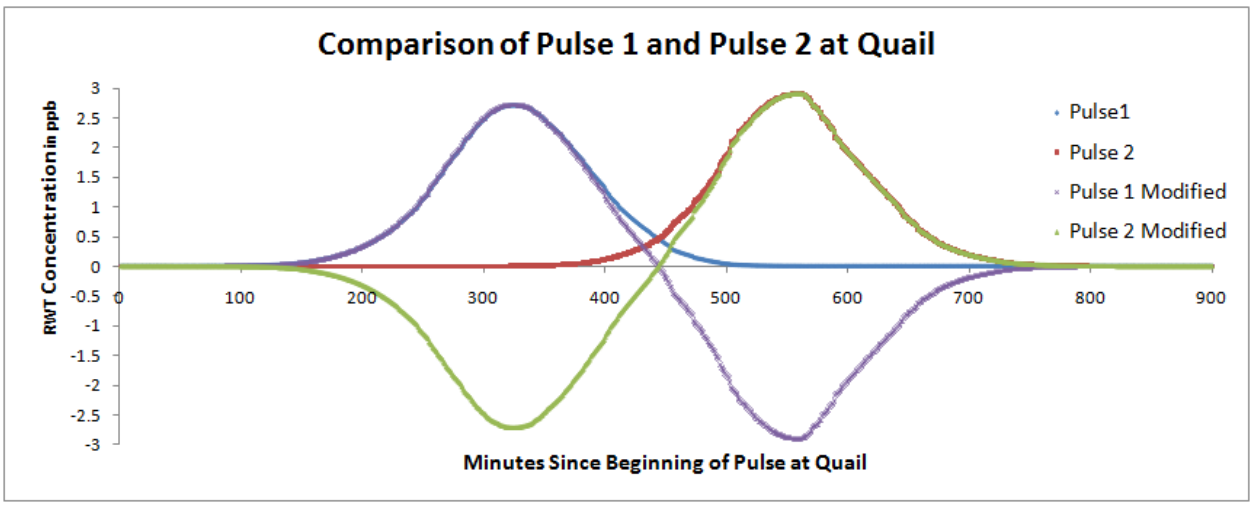

Figure 11: Scatterplot of RWT Pulses 1 and 2 at the Quail Bridge Sampling Site Showing Modeled Data of Each Pulse (in blue and red) and the Potential Influence Each Pulse Had on the Other Pulse (in purple and green)

The sheer velocities of each plume were calculated based on the travel times and the distances. These velocities are presented in feet per second in Tables 8 and 9. The velocities varied from 0.81 feet per second to 2.31 ft/s. In general, slower velocities were observed during daylight hours, and the fastest velocities were during the night hours. This is to be expected as the pumps run at night when electricity is less expensive and are shut off or throttled down when higher rates occur during the day. Due to dispersion we should observe velocities decreasing between the leading edge and trailing edge of each RWT plume. This was not the case between Parkhurst and Yuba during RWT pulse 1. The reasons for this will be discussed later in this report.

Table 8: Sheer Velocities for Leading Edge (V_l), Peak (V_p), 10% of Peak (V_{10p}), and Trailing Edge (V_t) of RWT Pulse 1

Velocity (in ft/s)	Ashlan	Brannon	Lincoln	Dinuba	Parkhurst	Yuba	Quail
V_l from O&M	1.96	2.24	2.02	1.81	1.84	1.49	1.48
V_p from O&M	1.63	1.92	1.71	1.54	1.48	1.40	1.39
V_{p10} from O&M	1.48	1.78	1.57	1.41	1.33	1.35	1.34
V_t from O&M	1.39	1.69	1.49	1.33	1.24	1.32	1.31
V_l from Ashlan		2.31	2.03	1.80	1.83	1.48	1.47
V_p from Ashlan		2.01	1.72	1.53	1.48	1.39	1.39
V_{p10} from Ashlan		1.87	1.58	1.41	1.33	1.35	1.34
V_t from Ashlan		1.78	1.50	1.33	1.24	1.32	1.31
V_l from Brannon			1.81	1.59	1.75	1.38	1.41
V_p from Brannon			1.51	1.34	1.39	1.32	1.34
V_{p10} from Brannon			1.38	1.22	1.24	1.29	1.30
V_t from Brannon			1.30	1.21	1.15	1.26	1.27
V_l from Lincoln				1.34	1.73	1.31	1.37
V_p from Lincoln				1.13	1.36	1.28	1.32
V_{p10} from Lincoln				1.04	1.21	1.27	1.29
V_t from Lincoln				1.09	1.12	1.25	1.27
V_l from Dinuba					1.87	1.31	1.37
V_p from Dinuba					1.43	1.31	1.34
V_{p10} from Dinuba					1.26	1.32	1.32
V_t from Dinuba					1.12	1.29	1.29
V_l from Parkhurst						0.81	1.18
V_p from Parkhurst						1.13	1.29
V_{p10} from Parkhurst						1.45	1.36
V_t from Parkhurst						1.84	1.42
V_l from Yuba							1.46
V_p from Yuba							1.37
V_{p10} from Yuba							1.32
V_t from Yuba							1.29

Table 9: Sheer Velocities for Leading Edge (V_l), Peak (V_p), 10% of Peak (V_{10p}), and Trailing Edge (V_t) of RWT Pulse 2.

Velocity (in ft/s)	Ashlan	Brannon	Parkhurst	Quail
V_l from O&M	1.85	1.79	1.40	1.49
V_p from O&M	1.63	1.56	1.32	1.39
V_{p10} from O&M	1.52	1.45	1.27	1.34
V_t from O&M	1.45	1.38	1.24	1.31
V_l from Ashlan		1.78	1.39	1.48
V_p from Ashlan		1.54	1.31	1.39
V_{p10} from Ashlan		1.43	1.26	1.34
V_t from Ashlan		1.36	1.23	1.31
V_l from Brannon			1.32	1.45
V_p from Brannon			1.26	1.37
V_{p10} from Brannon			1.23	1.33
V_t from Brannon			1.21	1.30
V_l from Parkhurst				1.62
V_p from Parkhurst				1.51
V_{p10} from Parkhurst				1.45
V_t from Parkhurst				1.41

A mean sheer velocity (V_m) was calculated for each RWT plume using an average of the V_l, V_p, and V_t for each reach. The V_m was always close to the V_p of each plume but not exactly. Table 10 Shows the V_m at each sampling site as calculated from the upstream station.

Table 10: Mean Sheer Velocities (V_m) for RWT Pulses 1 and 2

Velocity (in ft/s)	RWT Pulse 1	RWT Pulse 2
Mean Sheer Velocity (V_m) at Ashlan	1.66	1.64
Mean Sheer Velocity (V_m) at Brannon	2.03	1.56
Mean Sheer Velocity (V_m) at Lincoln	1.54	
Mean Sheer Velocity (V_m) at Dinuba	1.19	
Mean Sheer Velocity (V_m) at Parkhurst	1.47	1.26
Mean Sheer Velocity (V_m) at Yuba	1.26	
Mean Sheer Velocity (V_m) At Quail	1.37	1.51

The mean sheer velocity (V_m) at the time each pulse passed by each sampling site as found in Table 10 can be multiplied by the time it took for each RWT pulse to pass by each sampling site to get a sheer length in feet of each RWT pulse. This data is summarized in Table 11. The length of each RWT pulse should gradually increase as it travels downstream. The length of the plume at Parkhurst grew much more than would be expected. After the plume passed Parkhurst, the plume length shrank and began to look like it was gradually increasing from its length at Dinuba. It would not be physically reasonable for a RWT plume to shrink. The cause is due to unusual hydraulic conditions and will be discussed later in this report.

Table 11: Sheer Length (in feet) of RWT Pulses (d_s) for RWT Pulses 1 and 2

Sheer length (in feet)	RWT pulse 1	RWT pulse 2
Sheer length of RWT pulses (d_s) at Ashlan	3141.68	2176.63
Sheer length of RWT pulses (d_s) at Brannon	13873.46	12414.37
Sheer length of RWT pulses (d_s) at Lincoln	23612.28	
Sheer length of RWT pulses (d_s) at Dinuba	26362.66	
Sheer length of RWT pulses (d_s) at Parkhurst	80335.76	24422.06
Sheer length of RWT pulses (d_s) at Yuba	27211.43	
Sheer length of RWT pulses (d_s) At Quail	43965.76	51527.24

The longitudinal dispersion rates (K_d) for each location are listed in Table 12 and Table 13. The rates varied from about 0.61 ft/s to minus 2.03 ft/s. Negative values for K_d were not expected. The reasons for the negative dispersion rates will be discussed in detail later in the paper.

Table 12: Dispersion Rate, K_d, (in feet per second) of RWT Pulse 1

Dispersion rate K_d (ft/s)	Ashlan	Brannon	Lincoln	Dinuba	Parkhurst	Yuba	Quail
K_d from O&M	0.49	0.50	0.41	0.32	0.48	0.14	0.16
K_d from Ashlan		0.50	0.40	0.30	0.48	0.13	0.15
K_d from Brannon			0.32	0.24	0.47	0.08	0.12
K_d from Lincoln				0.12	0.51	0.03	0.09
K_d from Dinuba					0.62	0.01	0.09
K_d from Parkhurst						-2.03	-0.32
K_d from Yuba							0.19

Table 13: Dispersion Rate K_d (in feet per second) of RWT Pulse 2

Dispersion Rate K_d (ft/s)	Ashlan	Brannon	Parkhurst	Quail
K_d from O&M	0.35	0.36	0.15	0.18
K_d from Ashlan		0.37	0.14	0.18
K_d from Dinuba			0.09	0.16
K_d from Parkhurst				0.24

Reverse Flow in the California State Water Project

The data collected showed an anomaly at the Parkhurst Bridge sampling site. The travel times (t) from the leading edge to the trailing edge of each RWT pulse should have increased at each sampling site due to dispersion. At Parkhurst Bridge, the time of RWT pulse 1 to pass by the sampling site (delta time, Δt) increased greatly over the previous sampling sites. The Δt of RWT pulse 2 behaved similarly to RWT pulse 1 in three of four instances and diverged at Parkhurst as shown in Figure 12.

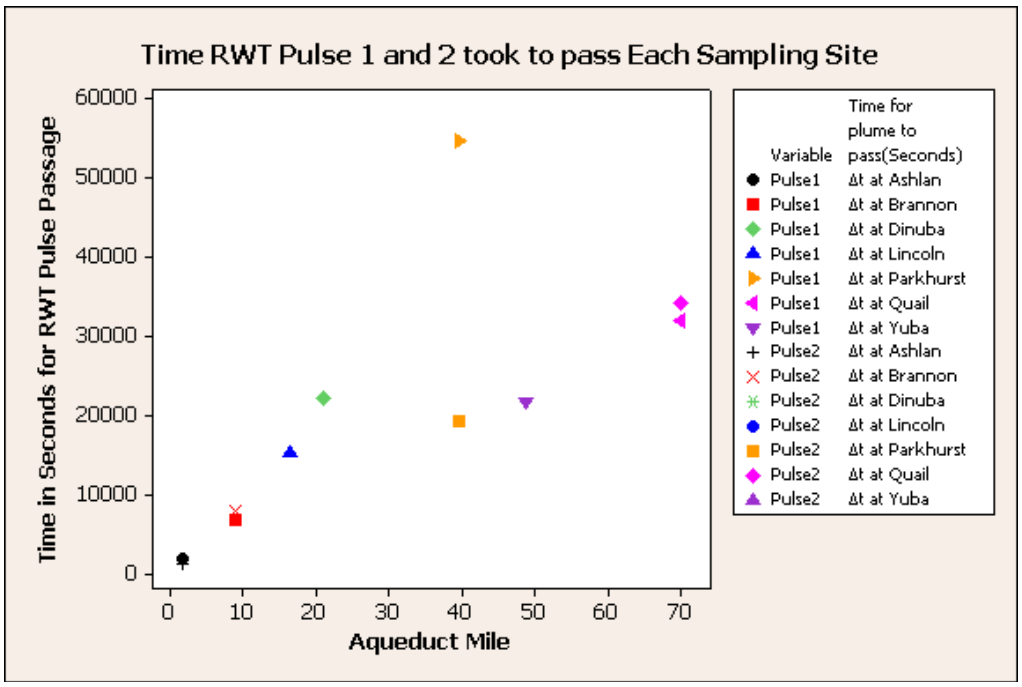

Figure 12: Scatterplot of Time for RWT Pulse 1 and 2 to Pass by Each Sampling Site

The mean sheer velocities at each sampling site varied within 2.1 ft/s and 1.1 ft/s. The aqueduct is operated at different flow rates depending on the price and availability of energy so velocity changes should be expected. These velocities are graphed in Figure 13.

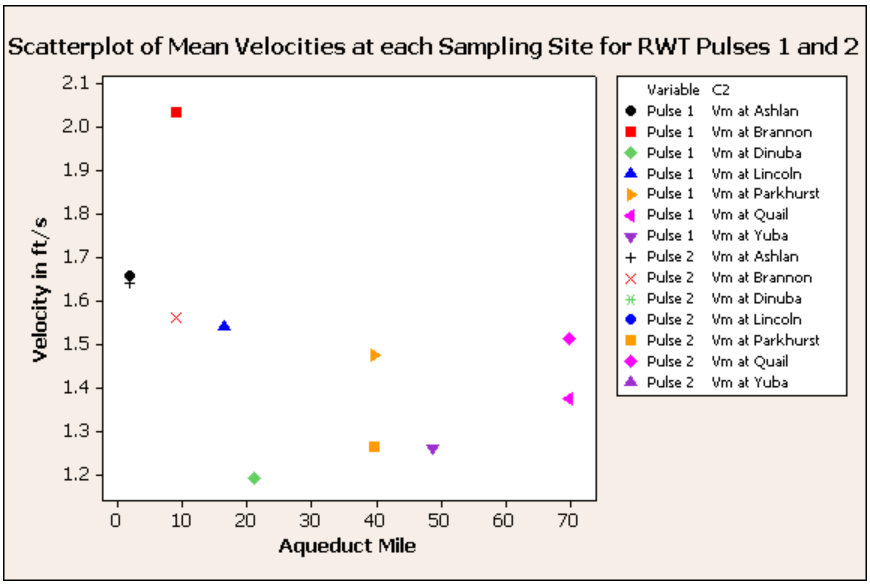

Figure 13: Scatterplot of Mean Velocities at Each Sampling Site for RWT Pulses 1 and 2

The dispersion rates (K_d, ft/s) of each RWT pulse calculated at each site are graphed in Figure 14. You can see that the calculated K_d is strongly negative for Yuba pulse 2. Negative dispersion would imply that the plume shrank after being stretched at the Parkhurst sampling site. This is physically impossible; however, it is a clue to explaining the particular anomaly observed at Parkhurst.

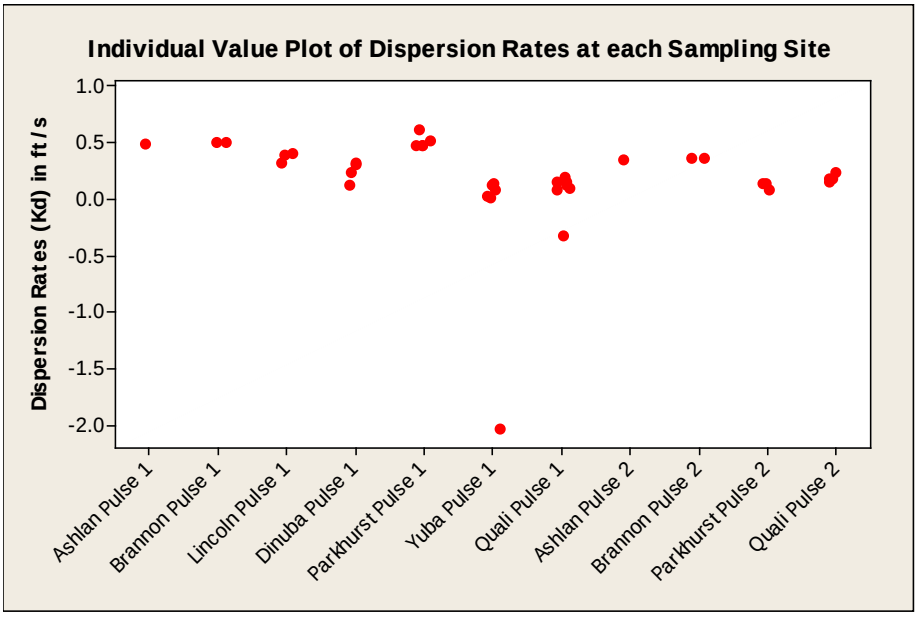

Figure 14: Individual Value Plot of the Dispersion Rates Calculated at Each Sampling Site for RWT Pulses 1 and 2

Observations of Flow Reversal

In spite of being a concrete-lined channel, the sides of the aqueduct are not absolutely smooth. The aqueduct has aquatic vegetation (macrophytes) growing on its sides below the low waterline. In calm water, macrophytes use various methods of flotation to maintain themselves in a vertical orientation. When the flow increases, the macrophytes lie flat against the bottom substrate due to the force of the water. During flow, the macrophytes are oriented with their tops pointing downstream.

During the investigation, the flow appeared to vary by a great deal during the day. At times, the flow was observed to be near zero; and the macrophytes oriented themselves vertically, indicating that there was very little to no flow. During times when there was little flow, schools of hundreds of carp, some over a meter in length, moved to the sides of the aqueduct to feed near the surface. On one occasion, the water level of the aqueduct appeared to be a few meters lower than usual. The macrophytes visible near the surface were pressed to the aqueduct lining, oriented with their tops pointed “upstream.” In this case, the flow in the aqueduct was moving upstream (reverse flow) rather than downstream.

The aqueduct has many turn-in and turn-out sites where water is taken from or added to the channel. DWR allots these withdrawals at weekly intervals and assigns a day of the week for each turn-out to pull water from the aqueduct. The meters on the turn-outs are read on a weekly basis to determine what each customer will be charged for the week. Apparently on the morning of Saturday, August 1, a turn-out upstream of the Parkhurst Bridge sampling site withdrew enough water to reverse the flows in the aqueduct and draw the water in pool 18 down to the macrophyte line.

Figure 15 shows the actual data for Parkhurst Bridge during RWT pulse 1. The smoothed RWT concentration data is in red, and the best fit Gaussian model of the data is in black. You can see that the measured data has two peaks. The investigators believe that this was due to a reversal in the flow of the aqueduct at around 09:00 hours August 1 until around noon of the same day. Based on an inflection in the curve, it appears the turn-out may have been drawing water from the aqueduct from about 06:00 hours. However, at the time between 06:00 and 09:00 hours, the aqueduct flow would have been greater than the turn-out flow. At noon, the turn-out would have either been turned off or the aqueduct's flow increased to greater than the flow of the turn-out. This anomaly elongated the RWT concentration pulse to where the pulse took nearly twice as long to pass the sampling site than at any other site. The model does not imitate what was recorded at all. The Pearson's rho for correlation at this sampling site was the lowest of all sites at 0.783 (see Table 4). Based on this anomaly, the dispersion rates that were calculated at Parkhurst and downstream for pulse 1 are unreliable due to the limited nature of the model.

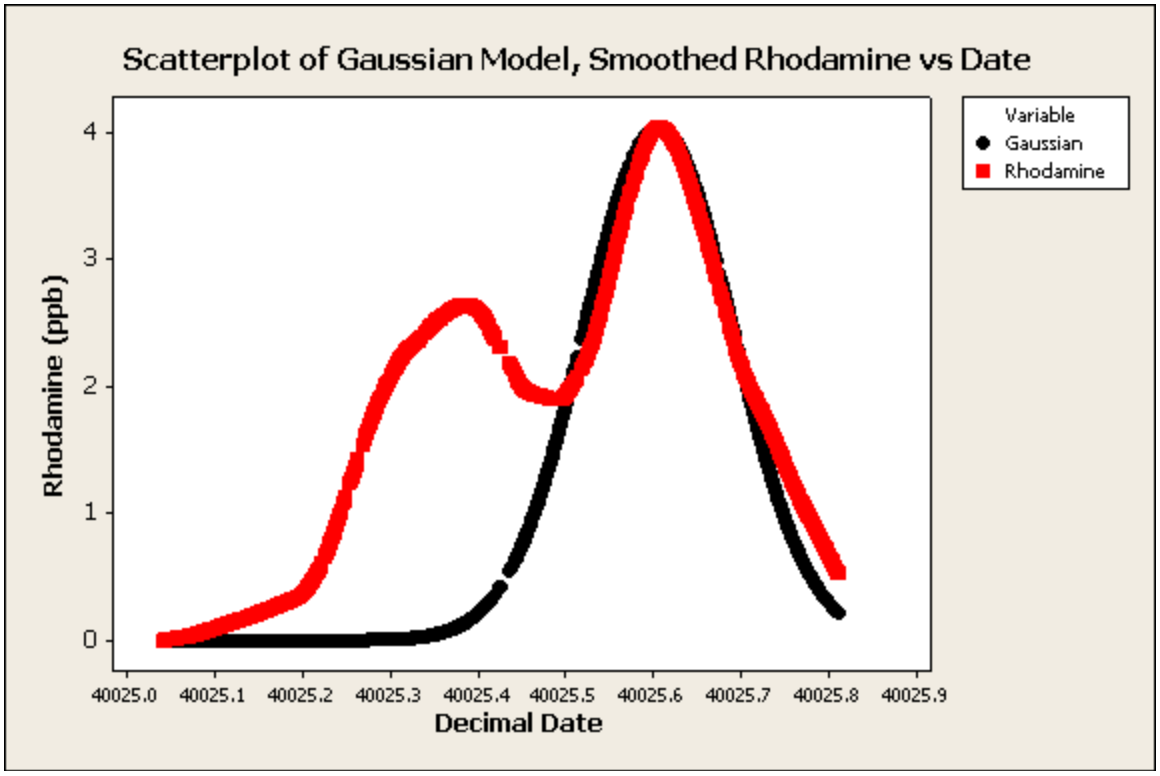

Figure 15: Scatterplot of Modeled RWT Concentration Data and Smoothed RWT Data over Time at Parkhurst Bridge during RWT Pulse 1

While the flow in the aqueduct was apparently moving upstream, a large amount of suspended solids were mobilized in the aqueduct creating a rise in turbidity that was detected by the turbidity sensors on the SCUFA device at Parkhurst Bridge (Figure 16). The suspended solids that cause turbidity settle to the bottom of the aqueduct as the turbulent conditions that mobilized them decrease in severity. Turbidity is not necessarily conserved as is RWT concentration as it travels down the aqueduct. The turbidity values at all other sampling sites were approximately 1 nephelometric turbidity unit (NTU) and varied by about 0.25 NTU around that value. The turbidity at Parkhurst rose as high as 3 NTU with much of the peak around 2 NTU with a variability of about 0.5 NTU. It took about 12 hours for the turbidity to return to normal background levels after suspended solids were mobilized.

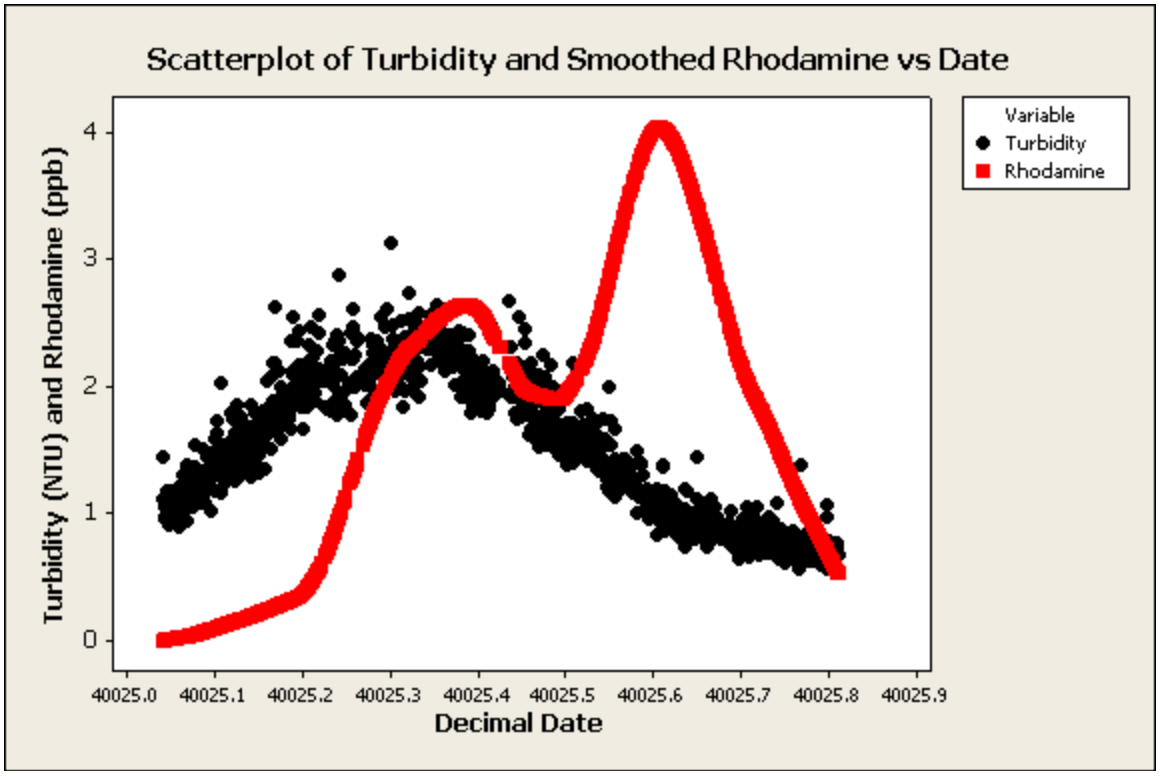

Figure 16: Scatterplot of Turbidity Data and Smoothed RWT Data over Time at Parkhurst Bridge during RWT Pulse 1

Conclusions

The California State Water Project Aqueduct is a trapezoidal concrete-lined channel that has flow regulated by pumping rates, which vary based on energy market conditions and water demand. The well-defined geometry should make the task of determining travel times and dispersion rates in the aqueduct simple compared to a riverine system. However, the aqueduct has certain characteristics that are unique to it. Water is added (pumped in) to the aqueduct by several entities at multiple points (turn-ins) for use at downstream locations (turn-outs). Municipal and agricultural users draw water from the aqueduct at multiple locations along the channel. These withdrawals and inputs of water are scheduled and monitored on a weekly basis, and actual flow conditions change on hourly time scales or less. This makes hourly or minute-to-minute predictions of use nearly impossible. At times, the aqueduct flow reverses direction when water withdrawals are greater upstream than the inputs into the system.

Travel Time

In spite of these difficulties, the study was able to give a good approximation of typical velocities in this stretch of the California State Water Project and provide estimates of typical longitudinal dispersion coefficients. Table 14 summarizes the statistical analyses of the velocity. Figure 17 is a boxplot of calculated velocities that shows the mean velocity in the reaches of this study is 1.501 ∓ 0.237 ft/s (mean $\mp$ standard deviation).

Table 14: Summary of Statistical Analyses of All Immediate Sheer Velocities Calculated from the Data Collected during the Study Period

Variable	N	Mean	Std. deviation	SE mean	95% confidence interval
Velocity	11	1.500 ft/s	0.237 ft/s	0.072	(1.341, 1.660)

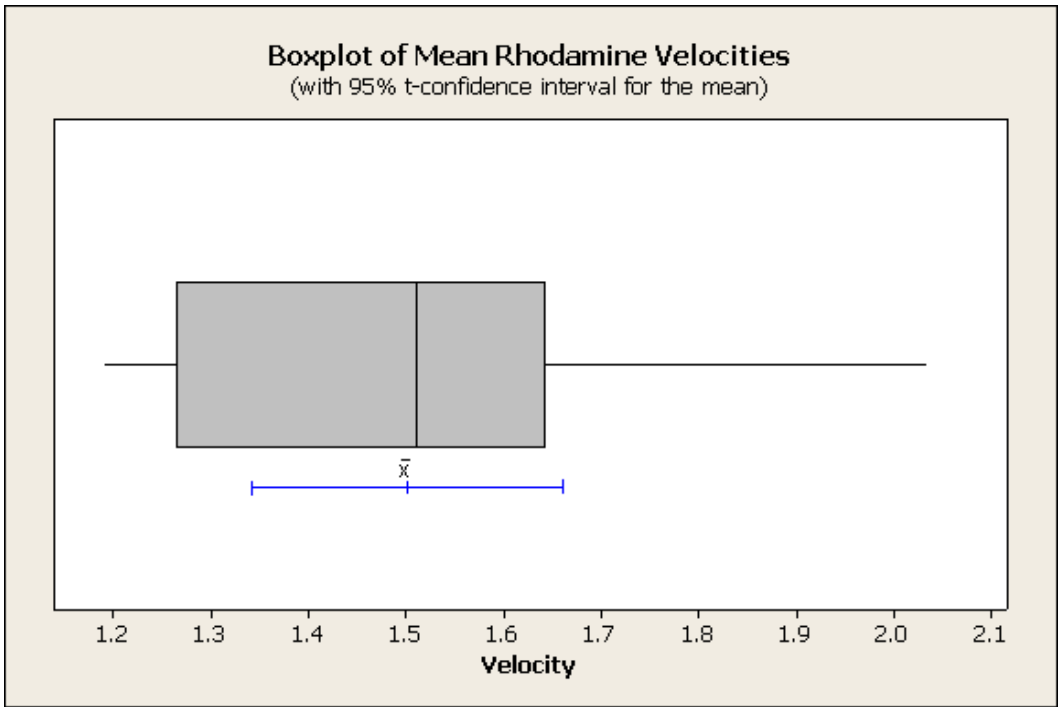

Figure 17: Boxplot of Statistical Analysis of Mean Velocities (ft/s)

Longitudinal Dispersion Rate

The dispersion rate calculation method was not able to account for discrepancies due to reverse flows in the aqueduct. Removing the sites that were affected by the anomaly of reverse flow allows us to get a good idea of what the dispersion is like in the aqueduct. With the anomalous data removed, the mean rate of dispersion, K_d, is 0.323 ft/s with a standard deviation of 0.134 ft/s. Table 15 summarizes the statistical analyses of the dispersion rate data. Figure 18 is a boxplot of both the clean data with the anomalous data from Parkhurst and Yuba removed and all the data including the anomalous data.

The boxplot of the dispersion rate data has a normal distribution, when considering only sites with non-anomalous data (see Figure18). The outlier of -2.034 ft/s would have changed the mean significantly and widened the confidence interval to include negative values, which are physically unrealistic.

Table 15: Summary of Statistical Analyses of the Dispersion Rates Calculated from the Data Collected during the Study Period

Variable	N	Mean (ft/s)	Std. deviation (ft/s)	SE mean (ft/s)	95% confidence interval (ft/s)
Dispersion rate (outlier removed)	8	0.323	0.134	0.047	(0.211, 0.435)
Dispersion rate all	11	0.114	0.731	0.220	(-0.377, 0.605)

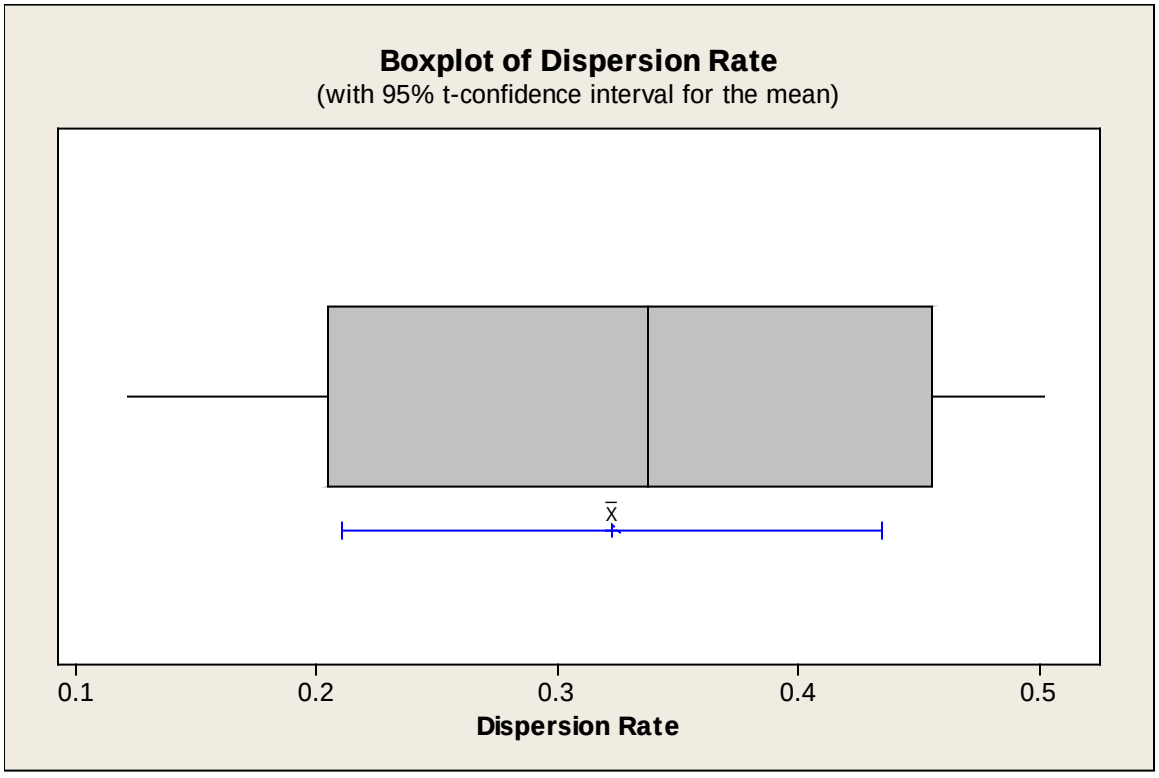

Figure 18: Boxplot of Statistical Analysis of Dispersion Rates

To our knowledge, this is the first study to measure travel time and longitudinal dispersion rate in the California Aqueduct. With these two parameters, velocity and dispersion rate, the questions posed by this study have been answered. Under conditions observed in this study, which are typical, average water velocity is 1.50 ft/s and the longitudinal dispersion rate is approximately 0.32 ft/s.

Example of the Usage

To better understand the usage of the water velocities and dispersion rates, an example is given below. A hypothetical incident involving a spill of atrazine into the aqueduct at Highway 33 utilizes calculations implemented in this study. Highway 33 crosses the aqueduct at mile marker 125.3. During the study period, there existed a great deal of variation in the water velocity in the aqueduct. The maximum velocity observed during the study period was 9,000 cfs, which is close to the typical maximum velocity observable in the system. The minimum observed water velocity was 3 to 5 cfs, which represents the minimum velocity of water in the aqueduct due to the natural slope of the aqueduct.

Travel speed

Under conditions similar to those in our study period, atrazine's average water velocity would be 1.50 ft/s or 1.023 mph with a standard deviation of 0.237 ft/s or 0.162 mph. In order to determine the likely fastest and slowest travel speeds of the peak, the 95% confidence interval is two standard deviations on either side of the average (the true travel speed is expected to fall within this range 95% of the time and expected to fall outside this range–either higher or lower–only 5% of the time). The fastest that atrazine would likely travel with 95% confidence would be 1.974 ft/s or 1.346 mph (calculation 1).

$$1.500\,\frac{ft}{s} + \left(2 * 0.237\,\frac{ft}{s}\right) = 1.974\,\frac{ft}{s}\ or\ 1.346\,mph \qquad \text{Calculation 1}$$

The slowest atrazine would likely travel with 95% confidence would be 1.026 ft/s or 0.700 mph (calculation 2).

$$1.500\,\frac{ft}{s} - \left(2 * 0.237\,\frac{ft}{s}\right) = 1.026\,\frac{ft}{s}\,or\ 0.700\,mph \qquad \text{Calculation 2}$$

Dispersion rate

Under conditions similar to those in our study, atrazine's average dispersion rate would be 0.323 ft/s or 0.220 mph with a standard deviation of 0.134 ft/s or 0.091 mph. To determine the likely boundary dispersion rates with 95% confidence, two standard deviations away from the average are used. The fastest atrazine would likely disperse with 95% surety would be 0.591 ft/s or 0.403 mph (calculation 3).

$$0.323\,\frac{ft}{s} + \left(2 * 0.134\,\frac{ft}{s}\right) = 0.591\,\frac{ft}{s}\ or\ 0.403\,mph \qquad \text{Calculation 3}$$

The slowest atrazine would likely disperse with 95% surety would be 0.055 ft/s or 0.038 mph (calculation 4).

$$0.323\,\frac{ft}{s} - \left(2 * 0.134\,\frac{ft}{s}\right) = 0.055\,\frac{ft}{s}\,or\ 0.038\,mph \qquad \text{Calculation 4}$$

The spill happens at time *t=0*, and we assume the atrazine spills into the aqueduct all at once. Twenty-four hours later, the portion of water with the highest concentration of the atrazine plume, or the peak concentration, would be expected to have traveled on average 24.54 miles (calculation 5).

$$24\ h * 1.023\,mph = \ 24.545\,miles \qquad \text{Calculation 5}$$

Maximum distances

The maximum distance the *peak* of the atrazine plume would be expected to travel with 95% surety is 32.302 miles (calculation 6).

$$24\ h * 1.346\ mph = \ 32.302\ miles \qquad \text{Calculation 6}$$

The *leading edge* of the atrazine plume would most likely be 5.280 miles ahead of the peak (calculation 7).

$$24\ h * 0.220\ mph = \ 5.280\ miles \qquad \text{Calculation 7}$$

The leading edge could have traveled farther than 5.280 miles. There is a 95% probability that the leading edge is within two standard deviations of the peak at 9.670 miles (calculation 8).

$$24\ h * 0.403\ mph = \ 9.670\ miles \qquad \text{Calculation 8}$$

Even though the spill most likely traveled only 29.825 miles downstream after 24 hours (calculation 9)

$$24.545\ miles + 5.280\ miles = 29.825\ miles \qquad \text{Calculation 9}$$

… to ensure containment of the spill, containment efforts initiated 24 hours after the incident would have to be at a point 41.972 miles downstream of the spill site (calculation 10).

$$32.302\ miles + 9.670\ miles = 41.972\ miles \qquad \text{Calculation 10}$$

Minimum distances

The peak of the atrazine plume could be as close to the spill site as 16.8 miles (calculation 11).

$$24\ h * 0.700\ mph = \ 16.800\ miles \qquad \text{Calculation 11}$$

The trailing edge of the plume could be as few as 7.13 miles from the spill site (calculation 12).

$$16.800\ miles - 9.670\ miles = 7.130\ miles \qquad \text{Calculation 12}$$

This is a large swath of 34.842 miles of water to be concerned about, where the spill responders can have 95% confidence of containing all of the spill (calculation 13; combining calculations 9 and 12).

$$41.972\ miles - 7.130\ miles = 34.842 \text{ miles} \qquad \text{Calculation 13}$$

An interesting characteristic in analyzing the imaginary atrazine spill is that the amount of atrazine spilled is irrelevant—the total mass does not affect the travel time and dispersion calculations. That is, dispersion rates and travel times do not depend on the initial starting *quantity* of a constituent.

Acknowledgements

The authors would like to thank the following individuals without whom this research would not be possible:

- Carol DiGiorgio, Gavin Dillon, Cindy Garcia, Cindy Messer, Eric Oppenheimer, and Dan Otis who gave mentoring and guidance that gave the project a clear vision.
- Otome Lindsey whose hands helped to move the research forward when obstacles blocked it.
- Arin Conner whose skill in engineering and fabricating made the installation of equipment appear easy.
- Singh Amardeep, Bryant Giorgi, Paul Hutton, Siquing Liu, Rich Losee, Dean Messer, Stephani Spaar, Bob Suits, and Dan Yamanaka who lent their expert eyes to review and refine this report.
- Mark Bettencourt, Sonia Miller, Murage Ngatia, and Steve San Julian whose elbow grease made the project move forward.
- Pam Borba, Alicia Luna, and Bob Mattos who served as guides in the San Luis Field Division.

Selected References

Ailsa Allaby and Michael Allaby. "dispersion." A Dictionary of Earth Sciences. 1999. *Encyclopedia.com.* 18 Oct. 2012 <http://www.encyclopedia.com>.

Cook, Sabrina M.F. and Dennis R. Linden. 1997. Use of Rhodamine WT to Facilitate Dilution and Analysis of Atrazine

Behrens, H. and G. Teichmann. 1982. Neue Ergebnisse über den Lichteinfluss auf Fluoreszenztracer. *In:* Tracer techniques in hydrology, Beitr. Geol. Schweiz-Hydrol., 28 (1)

Fischer, Hugo B., E. John List, Robert C.Y. Koh, Jorg Imberger, and Norman H. Brooks. 1979. Mixing in Inland and Coastal Waters. Academic Press. San Diego.

Hubbard, E.F., F.A. Kilpatrick, L.A. Martens, and J.F. Wilson Jr. 1982. Techniques of Water-Resources Investigations of the United States Geological Survey: Measurement of Time of Travel in Streams by Dye Tracing, Book 3, Chapter A9, Applications of Hydraulics.

Kilpatrick, F.A. 1970. Dosage Requirements for Slug Injections of Rhodamine BA and WT dyes. *In:* Geological Survey Research 1970: U.S. Geological Survey Professional Paper 700-B, p. 250-253.

Kilpatrick, F.A. and J.F. Wilson. 1989. Techniques of Water-Resources Investigations of the United States Geological Survey: Measurement of Time of Travel in Streams by Dye Tracing, Book 3, Chapter A9, Applications of Hydraulics.

NSF International. 2003 Oct 01. Drinking Water Treatment Chemicals - Health Effects Document Number: NSF/ANSI 60-2003e.

Suijlen, J.M. and J.J. Buyse. 1994. Potentials of photolytic rhodamine WT as a large-scale water tracer assessed in a long-term experiment in the Loosdrecht lakes. Limnol. Oceanogr., 39, 1411-1423.

U.S. Environmental Protection Agency (EPA). 1998. Announcement of the Drinking Water Contaminant Candidate List. Federal Register, Vol 63, No. 40, Mar 2 1998.

U.S. Food and Drug Administration (FDA). 1966. Policy Statement on Use of Rhodamine B Dye as a Tracer in Water Flow Studies: Department of Health, Education and Welfare, dated 22 April 1966